

Vehicle stability testing for flood flows

By G P Smith, B D Modra, T A Tucker and R J Cox

WRL TR 2017/07, May 2017



UNSW
Water Research
Laboratory



UNSW
SYDNEY

Water Research Laboratory
University of New South Wales
School of Civil and Environmental Engineering

Vehicle Stability Testing for Flood Flows

WRL Technical Report 2017/07

May 2017

by

G P Smith, B D Modra, T A Tucker and R J Cox

Project Details

Report Title	Vehicle Stability Testing for Flood Flows
Report Author(s)	G P Smith, B D Modra, T A Tucker and R J Cox
Report No.	2017/07
Report Status	Final
Date of Issue	1 May 2017
WRL Project Number	2016003
Project Manager	G P Smith
Client Name	NSW State Emergency Service, NSW Office of Environment and Heritage
Client Address	
Client Contact	SES, Belinda Davies belinda.davies@ses.nsw.gov.au OEH, Duncan Mcluckie duncan.mcluckie@environment.nsw.gov.au
Client Reference	

Document Status

Version	Reviewed By	Approved By	Date Issued
1 Draft	S Felder	G P Smith	23 March 2017
Final Draft	S Felder	G P Smith	19 April 2017
Final	S Felder	G P Smith	01 May 2017

Water Research Laboratory
110 King Street, Manly Vale, NSW, 2093, Australia
Tel: +61 (2) 8071 9800 Fax: +61 (2) 9949 4188
ABN: 57 195 873 179
www.wrl.unsw.edu.au
Quality System certified to AS/NZS ISO 9001:2008

Expertise, research and training for industry and government since 1959

Expertise, research and training for industry and government since 1959



A major group within
water@UNSW
water research centre

This report was produced by the Water Research Laboratory, School of Civil and Environmental Engineering, University of New South Wales for use by the client in accordance with the terms of the contract.

Information published in this report is available for release only with the permission of the Director, Water Research Laboratory and the client. It is the responsibility of the reader to verify the currency of the version number of this report. All subsequent releases will be made directly to the client.

The Water Research Laboratory shall not assume any responsibility or liability whatsoever to any third party arising out of any use or reliance on the content of this report.

Executive Summary

Every year floods cause enormous damage and loss of life on a global scale. An analysis of global statistics for loss of life showed that inland floods (river floods, flash floods and drainage floods) caused 175,000 fatalities and affected more than 2.2 billion people between 1975 and 2002 (Jonkman, 2005). More recent global analysis noted that 59,092 flood fatalities occurred worldwide between 2005 and 2014 (International Federation of Red Cross and Red Crescent Societies, 2015).

In a recent detailed analysis of flood fatalities in Australia, Haynes et al. (2016) noted that 1,859 people have died in floods since 1900 and that 178 of these flooding related deaths have occurred since 2000. The study noted that while flood fatality rates are generally falling per capita, the number of fatalities that occurred in vehicles, particularly four wheel drive (4WD) vehicles has increased in the last fifteen years.

Beyond the unfortunate occurrence of flood related fatalities, an enormous amount of time and resources are invested by emergency response organisations rescuing people who have entered floodwaters. Information sourced from the NSW SES website to the end of September 2016 indicates that nearly 550 flood rescues have been performed by NSW SES in 2016 alone (NSW SES, 2016). During the flooding of June 2016, NSW SES performed 300 flood rescues, approximately a third of which involved rescuing people from flooded vehicles (NSW SES, 2016).

It is clear that there is a need to better understand and quantify the mechanisms by which vehicles can become unstable in floodwaters. The research and analysis described in this report aims to improve the knowledge and information available to describe the vulnerability of vehicles as they enter floodwaters and to quantify the flow conditions that might cause vehicles to become vulnerable to being washed away. This knowledge can be used to better inform emergency managers and floodplain managers seeking to plan for, and respond to, flood emergencies.

This report describes an investigation of vehicle stability recently conducted at the UNSW Water Research Laboratory of the School of Civil and Environmental Engineering, UNSW Sydney. The report includes:

- A comprehensive literature review of pre-existing research and anecdotal evidence describing the vulnerability of vehicles in floodwaters;
- A description of the research scope;
- A description of the test methodology and test results;
- Discussion of the measured data;
- Interpretation of the data for use by decision makers in floodplain management and emergency planning.

Vehicle stability testing incorporated measurement of full prototype scale traction and buoyancy forces for threshold of movement of a vehicle in various depths of water in WRL's tow tank, and hydrodynamic force measurement on a 1:18 scale model vehicle to determine the equivalent hydrodynamic flow forces to reproduce the measured, full scale threshold of movement forces.

The traction force tests are considered novel in research on the stability of vehicles, and show that traction decreases rapidly with floodwater depths above the vehicle's floor pan level. The testing confirmed that the rear wheels (wheels not weighted by the engine) break traction far earlier than the front wheels.

Hydrodynamic testing showed that coefficients of drag for a vehicle in free surface water flows, perpendicular to the vehicle, are far higher than typical wind tunnel based aerodynamic drag coefficients. Flooded vehicle drag coefficients are consistent with the drag coefficients predicted by Hoerner (1965) for water surface piercing drag and are complicated by the vehicle geometry and low depth to vehicle length ratios. The coefficient of drag for a flooded vehicle varies non-linearly with the flow condition, but is generally within the range 1.2 and 2.0 for typical, dangerous flood conditions.

The test program and analysis presents a novel approach to the derivation of stability curves for vehicles in flood flows, by dissecting the forces that impact the vehicle, applying appropriate factors of safety for real-life flood conditions (as opposed to controlled laboratory conditions), and evaluating vehicle stability directly from the stability balance equation.

Observations from the testing confirm that where floodwaters impact the body of the vehicle, the vehicle is at greater risk of losing traction and being washed downstream. Flows that do not impact the body of the vehicle (hitting the wheels only) are generally considered safer for that vehicle.

Analysis of raw results from this investigation showed that the subject test vehicles were more stable in flood flows than the flood hazard vulnerability thresholds typically applied for floodplain management and emergency management as documented by guidelines such as Australian Rainfall and Runoff Review Project 10 (ARR P10) by Shand et al. (2011) and AEMI Handbook 7 (2014). However, mitigating factors described in this report, notably i) that the tested vehicles, while representative, were not the smallest and therefore the most vulnerable in their vehicle class and ii) that controlled laboratory conditions need to be interpreted to uncontrolled real life flood conditions meaning that a level of conservatism on this study's results is required. On this basis, the interim flood hazard threshold curves from ARR P10 summarised below for the two vehicle classes tested in this investigation are confirmed as appropriate for floodplain management and emergency planning.

Table ES-1: Proposed flood hazard thresholds for vehicle stability

Class of Vehicle	Length (m)	Kerb Weight (kg)	Ground Clearance (m)	Limiting Still Water Depth¹	Limiting High Velocity Flow Depth²	Limiting Velocity³	Equation of Stability
Small passenger	< 4.3	< 1250	< 0.12	0.3	0.15	3.0	$D.V \leq 0.3$
Large 4WD	> 4.5	> 2000	> 0.22	0.5	0.3	3.0	$D.V \leq 0.6$

¹ At velocity = 0 m/s; ² At velocity = 3 m/s; ³ At low depth

Regardless of these findings, it should be noted that estimation of the depth and velocity characteristics of floodwaters over a roadway in a real life flood emergency situations is fraught with difficulty. Floodwaters are often sediment laden and murky, making it difficult to assess the flow depth. In many cases, the flows overtopping flooded bridges or roadways may have been washed out below the floodwaters making the roadway unpassable. Without sophisticated equipment, flow velocities are notoriously difficult to assess, even to the trained eye. For these

reasons, the ad-hoc use of the above tabulated stability criteria by individuals in real flood situations to assess the safety of a road crossing is actively discouraged.

This report does not account for behaviour of drivers in flood emergencies, which remains a substantial factor in the ongoing loss of life in vehicles in floodwaters.

Having gained substantial knowledge of the vulnerability of vehicles exposed to floodwater, the authors of this report support the best advice of the Australian State Emergency Services to individual drivers which remains '**Never drive, ride or walk through floodwater**'.



Contents

Executive Summary	i
1. Introduction	1
2. Background: Vehicle Stability in Floodwaters	2
2.1 Vehicle stability information– literature review	3
2.1.1 Anecdotal evidence	9
2.1.2 Summary findings	10
3. Research Scope	11
4. Methodology	12
4.1 Overview	12
4.2 Formulation of the problem	14
4.2.1 Friction force of a vehicle	14
4.2.2 Hydrodynamic drag on a vehicle	16
5. Full Scale Vehicle Traction Tests	21
5.1 Overview	21
5.2 Test vehicles	21
5.3 Tyre coefficient of friction	23
5.4 Overview of traction tests	24
5.5 Test results	26
6. Hydrodynamic Force Testing (1:18 Scale)	32
6.1 Overview	32
6.2 Subcritical flows (tailwater controlled)	34
6.3 Critical flows (broad crested weir)	34
6.4 Supercritical flow (undershot gate)	35
6.5 Horizontal force testing results	36
7. Discussion of Results	39
7.1 Observations	39
7.2 Comparison of tested vehicles to other vehicles	41
7.3 Testing uncertainties	43
7.4 Interpretation of test information for floodplain management and emergency management	43
7.4.1 Preamble	43
7.4.2 Comparison with existing flood hazard curves	44
8. Conclusions	49
8.1 Recommendations	49
9. Acknowledgements	51
10. References	52

List of Tables

Table ES-1: Proposed flood hazard thresholds for vehicle stability	ii
Table 2-1: Proposed draft interim criteria for stationary vehicle stability (after Shand et al., 2011)	8
Table 4-1 Coefficient of Friction (adhesion) values between tyres and road surfaces, from Wong (1993)	15
Table 5-1: Vehicle specifications of prototype vehicles in present study	21
Table 5-2: Coefficient of friction results*	24
Table 5-3: Measured peak horizontal traction force results for the Toyota Yaris	29
Table 5-4: Measured peak horizontal traction force results for the Nissan Patrol	31
Table 6-1: Summary of Horizontal Force Testing (prototype)	36
Table 7-1 Comparison of smaller sized vehicle weights and dimensions	42
Table 7-2: Proposed flood hazard thresholds for vehicle stability	48

List of Figures

Figure 2-1: Combined flood hazard curves (after Smith et al., 2014; AEMI, 2014)	2
Figure 2-2: Vehicle stability failure mechanisms (after Shand et al., 2011)	3
Figure 2-3: Car floating in deep, slow flow https://www.youtube.com/watch?v=LC5ld79joIA (accessed 23 March 2017)	4
Figure 2-4: Car washed down an urban street in shallow, fast flow https://www.youtube.com/watch?v=3HrdgaiM9sY (accessed 23 March 2017)	5
Figure 2-5: 4WD utility washed off a causeway in Australia https://www.youtube.com/watch?v=Va8w7Jng9rM (accessed 22 March 2017)	5
Figure 2-6: Representation of all the results from literature (instability points and limit functions) obtained in experimental and theoretical studies (after Martinez-Gomariz et al., 2016)	8
Figure 2-7: Youtube footage of flooded cars in the Toowoomba floods of January 2010 (https://www.youtube.com/watch?v=kYUpkPTcqPY accessed 20 January 2017)	10
Figure 4-1: Schematic illustration of prototype scale test rig	12
Figure 4-2: Nissan Patrol in WRL's wave basin facility, preparing for a winch test from the rear axle	13
Figure 4-3: Slip curves for various road surfaces, extracted from Gerard (2006)	16
Figure 4-4 Drag coefficient of surface-piercing circular cylinders (on area d times h) as a function of Froude number, extracted from Hoerner (1965)	18
Figure 4-5 Drag coefficient of surface-piercing flat plates (on area b times h), extracted from Hoerner (1965)	19
Figure 4-6: Hoerner's (1965) formulation for surfacing piercing drag, extracted from Bowen et. al. (2011)	19
Figure 4-7: Flood flows over a causeway approaching Froude $Fr = 1$	20
Figure 5-1: Toyota Yaris in WRL's test facility, preparing for a winch test from both axles	22

Figure 5-2:	Nissan Patrol in WRL's wave facility, preparing for a winch test from the rear axle	22
Figure 5-3:	Winch assembly in WRL Lab#2, including (a) framework, winch and dynamometer, (b) pulley and wheel attachment	23
Figure 5-4:	Rapid filling of WRL's test tank (wave basin). The winch assembly is also shown.	25
Figure 5-5:	Toyota Yaris in WRL's wave basin facility, in 0.6 m water depth with rear wheels clear of the floor	26
Figure 5-6:	The lead author demonstrating zero traction at the rear wheels for the Nissan Patrol 4WD in WRL's Lab#2 testing tank. Water depth is approximately 1.0m.	26
Figure 5-7:	Traction force time series for tests on the Toyota Yaris with one driver occupant, winched from the rear axle only	27
Figure 5-8:	Traction force time series for tests on the Toyota Yaris with four occupants, winched from the rear axle only	28
Figure 5-9:	Traction force time series for tests on the Toyota Yaris with one driver occupant, winched from both axles	28
Figure 5-10:	Traction force time series for tests on the Nissan Patrol with one driver occupant, winched from the rear axle	29
Figure 5-11:	Measured peak horizontal traction force for a Toyota Yaris 2006 in varying static water levels. Tests were conducted on three scenarios with varying passenger loads and tow points	30
Figure 5-12:	Measured peak horizontal traction force for a Nissan Patrol 4WD 1998, winched from the rear axle only, with one occupant	31
Figure 6-1:	Test assembly for testing of the horizontal hydrodynamic forces. Flow is from the left of the picture	33
Figure 6-2:	Testing of the model in subcritical flows: $Fr = 0.3$, $d = 0.71m$, $v = 0.80m/s$ (prototype)	34
Figure 6-3:	Testing of the model on a broad crested weir	35
Figure 6-4:	Testing of the model in supercritical flows $d = 0.225m$, $v = 4.0m/s$ (prototype), $C_D = 1.86$, $Fr = 2.66$	36
Figure 6-5:	Coefficient of Drag for a Toyota Yaris based on the horizontal hydrodynamic force tests	38
Figure 7-1:	Vehicle stability deduced from prototype scale measurements - rear wheel horizontal force thresholds versus water depth	39
Figure 7-2:	Comparison of the Force vs Depth relationship for the Hydrodynamic Tests and the Winch Tests; Toyota Yaris	41
Figure 7-3:	Stability Curve for a Toyota Yaris based on full scale traction tests, upper limits for the Coefficient of Drag $C_D = 2.0$ based on scale testing, and points scaled to a flood condition Coefficient of Friction of 0.3	45
Figure 7-4:	Stability Curve for a Nissan Patrol based on full scale traction tests, upper limits for the Coefficient of Drag $C_D = 2.0$ based on scale testing, and points scaled to a flood condition Coefficient of Friction of 0.3	46

1. Introduction

Every year floods cause enormous damage and loss of life on a global scale. An analysis of global statistics for loss of life showed that inland floods (river floods, flash floods and drainage floods) caused 175,000 fatalities and affected more than 2.2 billion people between 1975 and 2002 (Jonkman, 2005). More recent global analysis noted that 59,092 flood fatalities occurred worldwide between 2005 and 2014 (International Federation of Red Cross and Red Crescent Societies, 2015).

In a recent detailed analysis of flood fatalities in Australia, Haynes et al., (2016) noted that 1,859 people have died in floods since 1900 and that 178 of these flooding related deaths have occurred since 2000. The study noted that while flood fatality rates are generally falling per capita, the number of fatalities that occurred in vehicles, particularly four wheel drive (4WD) vehicles has increased in the last fifteen years.

When discussing flood fatalities, Haynes et al., (2016) also notes:

- That the greatest proportion of flood related fatalities occurred while the person was attempting to cross a bridge causeway or road, whether the person was in a vehicle or on foot;
- Most victims were capable of independent action (not impaired in any way e.g. by alcohol consumption) and aware of the flood, however the speed and depth of the water took them by surprise.

Beyond the unfortunate occurrence of flood related fatalities, an enormous amount of time and resources are invested by emergency response organisations rescuing people who have entered floodwaters. Information sourced from the NSW SES website to the end of September 2016 indicates that nearly 550 flood rescues have been performed by NSW SES in 2016 alone (NSW SES, 2016). During the flooding of June 2016, NSW SES performed 300 flood rescues, approximately a third of which involved rescuing people from flooded vehicles (NSW SES, 2016).

It is clear from this brief introduction that there is a need to understand the mechanisms by which vehicles become unstable in floodwaters. The research and analysis described in this report aims to improve the knowledge and information available, to describe the vulnerability of vehicles as they enter floodwaters and to quantify the flow conditions that might cause vehicles to become vulnerable in floodwaters. This knowledge can be used to better inform emergency managers and floodplain managers seeking to plan for, and respond to, flood emergencies.

2. Background: Vehicle Stability in Floodwaters

Baseline information on the stability of vehicles in floodwaters is used by floodplain managers and emergency managers to support important planning decisions. Vehicle stability information can be used in various ways, but typically it is used to quantify and classify the vulnerability of vehicles when exposed to floodwaters. One pertinent example of the use of vehicle stability information is illustrated in Figure 2-1. This figure shows a set of flood hazard¹ threshold curves used to classify the vulnerability of a community exposed to flood. The figure is based on the premise that people can be vulnerable in three general locations on a floodplain: on foot; in a vehicle; or in a building (Smith et al., 2014, AEMI, 2014; Haynes et al., 2016). Figure 2-1 shows that for a given flow velocity, flood hazard increases with increasing flow depth and that for a given flow depth the flood hazard increases with increasing flow velocity. Often the vulnerability of people and infrastructure on a floodplain is expressed as product of velocity V and flow depth D ($V \cdot D$ values).

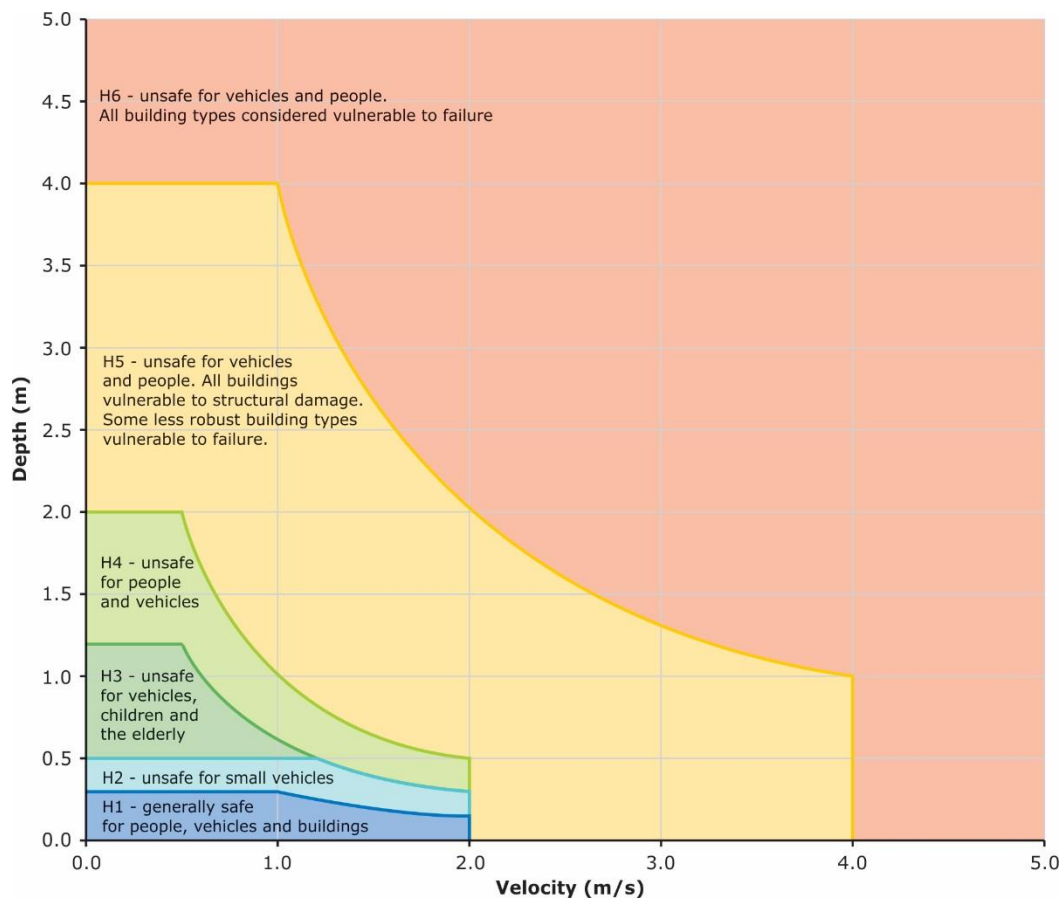


Figure 2-1: Combined flood hazard curves (after Smith et al., 2014; AEMI, 2014)

Vehicle stability thresholds expressed in the form illustrated in Figure 2-1 or similar can be applied in various ways. In a generic sense, the information can be applied to support decisions where vehicular access to a potentially flooded area might need to be controlled or restricted. For example, an emergency manager might use the thresholds to classify available flood

¹ Flood Hazard: Potential loss of life, injury and economic loss caused by future flood events. The degree of hazard varies with the severity of flooding and is affected by flood behaviour (extent, depth, velocity, isolation, rate of rise of floodwaters, duration), topography and emergency management.

mapping in order to define a safe vehicle evacuation route or the information might be used to support guidance on when a particular causeway or roadway crossing a stream or floodplain might need to be closed to traffic. The information could also be used to support an education campaign to inform community members of the dangers of driving through flood waters.

2.1 Vehicle stability information– literature review

The UNSW Water Research Laboratory (WRL) has previously conducted a literature review of vehicle stability as Australian Rainfall and Runoff Review Project 10 (ARR P10) (Shand et al., 2011). Readers are directed to this review for a detailed summary of various referenced documents.

This report section summarises the ARR P10 review, but has been extended with references published in the intervening period.

There are essentially three reasons why vehicles are vulnerable in floodwaters:

- Though many 4WD vehicles are designed to be driven in water, the reality is that for many vehicles, entering water causes the engine to stop, preventing the vehicle from being driven further into, or out of the water by the driver;
- The vehicle floats; and
- The vehicle becomes difficult to control.

The safety of people during flood events can be compromised when vehicles they are travelling in are exposed to flood flows which cause the vehicle to become unstable by losing traction (frictional instability through sliding), to topple because of uneven surfaces or to become buoyant (floating). These mechanisms can lead to a complete loss of control over the vehicle resulting in the vehicle being swept downstream (Shand et al., 2011; Haynes et al., 2016). These stability failure mechanisms are illustrated in Figure 2-2.

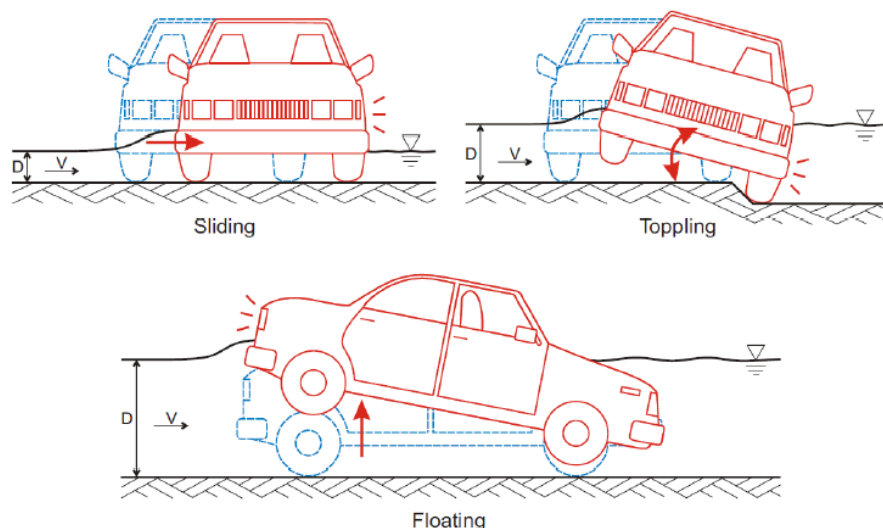


Figure 2-2: Vehicle stability failure mechanisms (after Shand et al., 2011)

A distinction should be made between flow-induced stability loss and stability loss induced by the interaction of a vehicle at high speed and evenly distributed water, commonly referred to as hydroplaning (Gallaway et al., 1979). This phenomenon is of concern for vehicle stability but generally occurs at high vehicle speeds and at low water depth. Hydroplaning is therefore not considered further within this study.

Once the flow thresholds for vehicle stability have been exceeded (Figure 2-1) and the vehicle becomes unstable, the vehicle will typically be moved by the force of the water in the direction of flow and observations of video footage of actual floods demonstrate that the vehicle often then drifts under the influence of the floodwaters into deeper, faster moving, more dangerous flow. Figures 2-3 to 2-5 (and the linked videos) illustrate situations where vehicles floated in deep subcritical flood waters or were swept away by supercritical flood waters with high flow velocity and relatively low flow depth.



Figure 2-3: Car floating in deep, slow flow

<https://www.youtube.com/watch?v=LC5ld79joIA> (accessed 23 March 2017)



Figure 2-4: Car washed down an urban street in shallow, fast flow
<https://www.youtube.com/watch?v=3HrdgaiM9sY> (accessed 23 March 2017)



Figure 2-5: 4WD utility washed off a causeway in Australia
<https://www.youtube.com/watch?v=Va8w7Jng9rM> (accessed 22 March 2017)

The weight distribution in most vehicles is uneven with a greater proportion of the weight located near the engine. In most vehicles, this means that the rear of the vehicle floats first (as illustrated in Figure 2-2) with the front wheels below the engine remaining on the ground for longer. Where floodwaters have adequate velocity, the rear of the vehicle is prone to swing around, pivoting on the front wheels until the vehicle is aligned with the flow direction.

While there is general agreement on the mechanisms for vehicle instability (Figure 2-2), a collation of literature on the flow conditions which induce vehicle instability notes a wide range of values. Shand et al., (2011) highlights that guidelines provided for vehicle stability on floodways have generally been based on the product of depth and velocity, as derived by scaled experimental investigations of stationary vehicle stability. Shand et al., (2011) provides a comprehensive summary of literature published prior to 2010. These studies, highlighted substantial changes in vehicle design since the original studies of vehicle stability by Bonham and Hattersley (1967) and Gordon and Stone (1973) which have been used as the basis of flood hazard policy in Australia. There was no significant research published in this field of vehicle stability in the intervening period between Gordon and Stone's work in 1973 and Shand et al.'s literature review in 2011.

More recent investigations of vehicle stability are not included in the review by Shand et al., (2011). Recent experimental investigations have been undertaken using scale model die-cast vehicles in a horizontal hydraulic flume at the Hydro-environmental Research Centre of Cardiff University, United Kingdom (Shu et al., 2011; Xia et al., 2011). These studies evaluated the theoretical forces exerted on a fully submerged and static vehicle under flow conditions to derive an expression for the instability threshold. The drag and frictional coefficients were included implicitly within the expression and derived by laboratory flume testing using model vehicles. This methodology differed from previous studies, where reaction forces were measured for a geometrically scaled vehicle subject to flows and the instability threshold was calculated for various coefficients of friction.

Xia et al., (2011) tested three types of vehicle using an initial geometric scale of 1:43 with verification tests at a larger 1:18 scale. Shu et al. (2011) tested the same three vehicle types namely Mitsubishi Pajero, BMW M5, Mini Cooper, undertaking all tests at 1:18 scale. Both testing programs assumed all wheels to be locked and the vehicle orientated parallel to the flow direction. Velocity was increased for a given depth until vehicle motion was initiated. Experimental results were used to calibrate the parameters within the theoretical expression for instability thresholds.

The studies differed in that Xia et al., (2011) did not correctly scale the vehicle density, and therefore mass of the model vehicles, according to dynamic similarity principles but rather used a relative density term in the analytical solution to adjust the measured data to match the prototype. The resultant values of Xia et al. (2011) differed significantly from other studies (by up to an order of magnitude) with vehicles becoming submerged before moving and were inconsistent with qualitative evidence from the field (i.e. during the Queensland floods in February 2011 (<https://www.youtube.com/watch?v=kYUkpPTcqPY> accessed 24 March 2017) and the Japan Tsunami in March 2011 (<https://www.youtube.com/watch?v=7trfmf5SuQs> accessed 24 March 2017) where cars floated well before they became submerged).

Shu et al., (2011) correctly scaled the density and mass of model vehicles and obtained D.V values slightly higher than those found in earlier investigations. Shu et al., (2011) had the model test vehicles filled with foam to resist ingress of water. This was thought to better represent modern vehicles with significantly improved dust seals than the older cars tested in most other investigations. Shu et al., (2011) determined the friction coefficients to range from 0.39 to 0.68 for their models, quoted to be within prototype ranges given by Gerard (2006). The differences in stability thresholds noted in Shu et al., (2011) are likely due to the higher coefficient of friction in the Shu et al., (2011) models ($\mu = 0.39$ to 0.68) compared to the lower friction coefficients ($\mu = 0.3$) adopted by earlier studies (e.g. Bonham and Hattersley, 1967; Keller and Mitsch, 1992). Sensitivity testing of Shu et al., (2011) using a reducing frictional

coefficient ($\mu = 0.5$) gave lower critical D.V values and may tend toward those found in earlier studies. The authors of Xia et al., (2011) and Shu et al., (2011) acknowledge that in prototype vehicles, mass is not evenly distributed leading to the rear of a vehicle often floating first. This prevents the rear wheels from contributing friction to prevent motion. The model vehicles have more evenly distributed mass and therefore do not accurately represent this occurrence and may therefore overestimate the friction resistance of vehicles.

Shu et al., (2011) verified their results against two field observations of cars moving during flood events. The threshold of vehicle motion and the flow rate, which may be considered safe for vehicle passage are likely to be lower than values observed for vehicles already moving in flood flow.

Toda et al., (2013) also completed scale model testing of a sedan at 1:10 scale and a minivan at 1:18 scale in a 1 m wide flume. Froude similarity principles were used for scaling. Considerable effort was invested in adequately representing the weight distribution between front and rear of the vehicles and buoyancy of the scale models. Models were tested with the vehicle oriented so the vehicle pointed into the direction of flow (0 degree) and oriented across the flow (90 degree) to determine instability. Friction coefficients were measured at both 0 and 90 degree orientation to the flow with friction values of 0.26 and 0.57, respectively, for the sedan and friction coefficients of 0.42 and 0.65 for the minivan. The authors provided a simplified conclusion that cars would move in floodwaters greater than 0.5 m deep and flowing at a velocity greater than 2 m/s.

Martínez-Gomariz et al., (2016) provided an excellent compilation of all previous literature including a graphical comparison of all available experimental and theoretical results. The graphical comparison is reproduced in Figure 2-6. A comparison with the findings of these experimental studies shows the vehicle stability threshold data proposed by Shand et al., (2011) and adopted by Australian Rainfall and Runoff and the Australian Emergency Management Institute (AEMI, 2014) for flood hazard estimates are conservative compared to the compiled data sets.

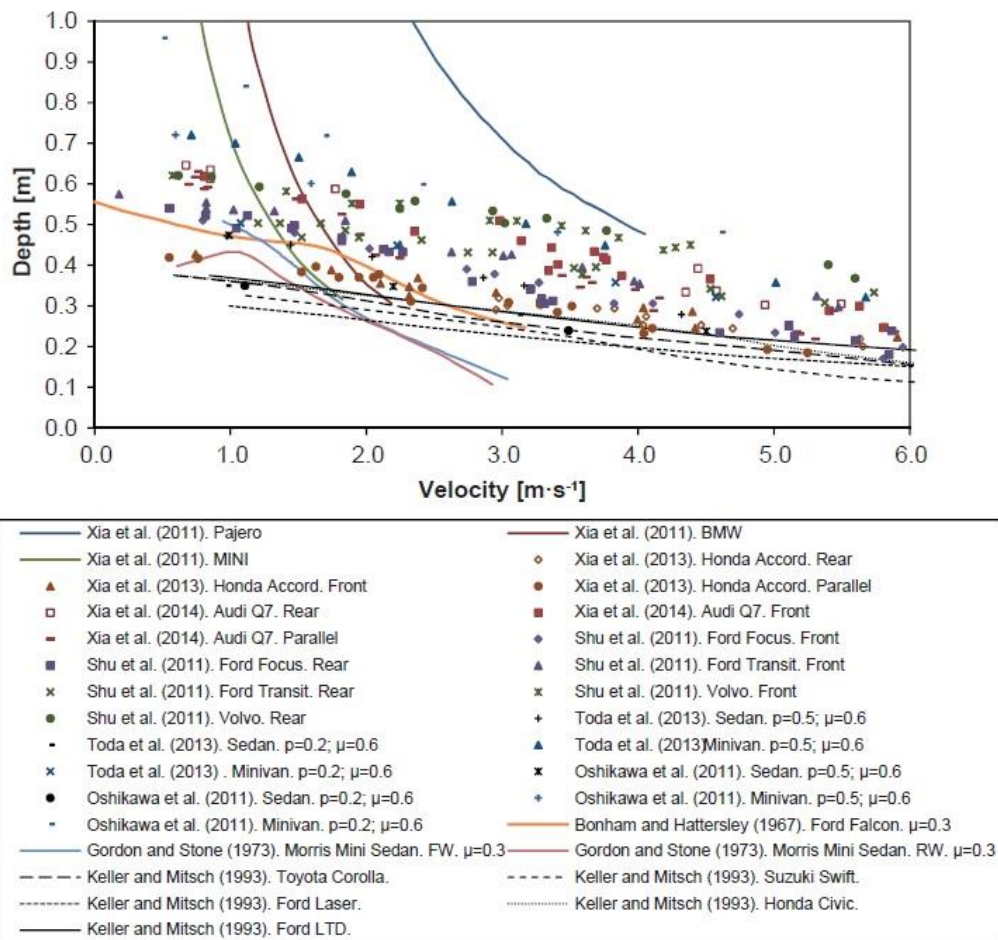


Figure 2-6: Representation of all the results from literature (instability points and limit functions) obtained in experimental and theoretical studies (after Martinez-Gomariz et al., 2016)

The criteria proposed by Shand et al., (2011) presented in Table 2-1 have taken into consideration the safety criteria for people (Cox et al., 2010), ensuring that, in event of vehicle failure, safety was not compromised once people abandoned their cars.

Table 2-1: Proposed draft interim criteria for stationary vehicle stability (after Shand et al., 2011)

Class of Vehicle	Length (m)	Kerb Weight (kg)	Ground Clearance (m)	Limiting Still Water Depth ¹	Limiting High Velocity Flow Depth ²	Limiting Velocity ³	Equation of Stability
Small passenger	< 4.3	< 1250	< 0.12	0.3	0.1	3.0	$D.V \leq 0.3$
Large passenger	> 4.3	> 1250	> 0.12	0.4	0.15	3.0	$D.V \leq 0.45$
Large 4WD	> 4.5	> 2000	> 0.22	0.5	0.2	3.0	$D.V \leq 0.6$

¹ At velocity = 0 m/s; ² At velocity = 3 m/s; ³ At low depth

Importantly, Shand et al., (2011) highlighted and Martinez-Gomariz et al., (2016) agreed, that the available scaled experimental data is being applied beyond its limits, and that the criteria are unlikely reliable enough to be adopted permanently as safety criteria. Shand et al., (2011) noted particularly that this is due to the data not allowing adequate assessment of:

- Appropriate coefficients of friction for use in flood flows;
- Buoyancy of modern cars;
- The effect of vehicle orientation to flow direction (including vehicle movement); and
- Information for additional categories including small and large commercial vehicles and emergency service vehicles.

Many of the studies listed above, particularly Shand et al., (2011), Xia et al., (2011) and Shu et al., (2011) recommended full scale testing to investigate thresholds of flooded vehicles under real and more complex circumstances.

2.1.1 Anecdotal evidence

The internet, particularly web sites such as *youtube.com*, provides a wealth of documented anecdotal observations of vehicles in floodwaters. Internet video footage sampled as part of this research generally validates the conclusion of Haynes et al., (2016) that vehicles most commonly come into contact with floodwaters when they are deliberately driven into floodwaters, either at a bridge or causeway crossing.

Observations of vehicles in these circumstances show that most commonly the vehicle enters the flood waters with flow passing perpendicular to the vehicle direction, i.e. the road or causeway that is being overtopped by floodwater is more or less perpendicular to the flow direction. This is generally the worst orientation for vehicle stability as it provides the greatest vehicular cross-sectional area to the flow, and therefore the highest possible hydrodynamic flow force is applied to the vehicle.

Video footage also demonstrates, that in this scenario, the most common mode of failure is for the vehicle's rear wheels to lose traction causing the vehicle to rotate nose first into the flow and in many cases then be washed off the roadway into deeper water as illustrated in Figure 2-7.

This mode of failure is reasonably anticipated since the typical configuration of modern vehicles is with a forward mounted engine, in front of a near water-tight cabin and boot/trunk rearwards of the rear axle. As the vehicle becomes inundated, the rear of the vehicle is more buoyant than the front with less downwards force due to the vehicle weight at the rear wheels. Less weight over the rear axle means less friction available from the tyres, and so the rear wheels break traction first.

If the rear wheels break traction in moving floodwaters, the vehicle has a tendency to pivot on the front wheels eventually pointing the front of the vehicle into the direction of flow. If the vehicle remains on a reasonably flat surface, then with water pressure sometimes rising over the bonnet of the vehicle, the vehicle may become more stable and stop moving. However, in many recorded instances the vehicle rolls off the road over the edge of a causeway or bridge, or may simply roll away downstream. *For this reason, the point of instability of the vehicle is defined in this study as the point at which any axle (two wheels) loses traction and the vehicle rotates or translates sideways.*



Figure 2-7: Youtube footage of flooded cars in the Toowoomba floods of January 2010
(<https://www.youtube.com/watch?v=kYUpkPTcgPY> accessed 20 January 2017)

2.1.2 Summary findings

The review of currently available literature concluded that there are a number of limitations to the previous research on vehicle stability in floodwaters, including:

- There is currently no full scale testing of the stability of vehicles in floodwaters;
- Only one test program considered testing of the forces on a vehicle at full scale (Kramer et. al., 2016), but this suffered from ingress of water into the vehicle, and ignored the effect of changing vehicle height and aspect/tilt due to unloading of the springs.
- No validation of the limit to model scaling has been conducted. It is likely that scales smaller than 1:20 will be undermined by scale effects. Even at larger scales some forces, such as surface tension, may affect the results.
- The orientation of the vehicle in some studies is not particularly relevant to the exposure of the risk to life of people in vehicles which encounter floodwaters. Evidence presented shows that vehicles driven into floodwaters most commonly do so perpendicular to the direction of travel.
- Testing of fully submerged vehicles is not relevant to risk to life in vehicles exposed to floodwaters as the vehicle would need to be fully flooded, which is clearly a hazard for any occupants.

Little previous work has aimed to separate and understand the various forces that act on a vehicle in floodwaters. This limits the ability of the scientific community to study specific aspects of vehicle stability in detail, such as buoyant behaviour, tyre-road friction or hydrodynamic forces. This limits the ability to determine uncertainty in testing programs, or develop suitable factors of safety, and to recommend defensible parameters to use in floodplain management or emergency management and operations when considering vehicular access in flood prone areas.

3. Research Scope

The research scope for this project was driven by the need to better understand and quantify the mechanisms by which vehicles become unstable in floodwaters. By better understanding the stability limits of vehicles in flood flows, and quantifying the flow conditions that might cause vehicles to become vulnerable to being washed away by floodwaters, better informed emergency managers and floodplain managers can more effectively plan for, and respond to, flood emergencies.

The research and analysis described in this report aims to improve the knowledge and information available. The study aims were to:

1. Determine the likely conditions in which a vehicle may be washed away in floods;
2. Determine the buoyant behaviour of vehicles and the subsequent impact on road-tyre friction by direct measurement of a sample of full scale vehicles in water;
3. Determine the hydrodynamic forces on a vehicle and the vehicle's coefficient of friction by scale physical modelling;
4. Develop a method of analysing vehicle stability in floodwaters that allows component forces to be considered and allows a robust approach to evaluating uncertainty in the results;
5. Based on the results of testing the friction and hydrodynamic forces, as well as other available literature, determine suitable stability curves for passenger vehicles and large 4WD vehicles.

Direction for the research scope was also derived from the key findings of Haynes et al. (2016) that:

- The greatest proportion of flood related fatalities occurred while the person was attempting to cross a bridge, causeway or road, whether the person was in a vehicle or on foot;
- Most victims were capable of independent action (not impaired in any way e.g. by alcohol consumption) and aware of the flood, however the speed and depth of the water took them by surprise.

The following research scope was proposed to address these primary research needs:

- i. Measure the stability of vehicles when exposed to floodwaters at prototype (full) scale using real vehicles;
 - a. Devise tests that are representative of typical scenarios where vehicles on bridges or causeways have been washed away in floodwaters;
- ii. Based on these measurements, review the flood hazard vulnerability criteria for flood exposed vehicles.

4. Methodology

4.1 Overview

The overriding limitation with currently available research of vehicle stability is that all previous research assessment has been conducted at model scale. A particularly novel aspect of this current research is the world first, direct measurement of the forces required to cause a passenger vehicle to become unstable in floodwaters at full scale.

The test methodology was designed to separate the response of the vehicle exposed to floodwaters to both friction and hydrodynamic forces. Two rounds of testing were completed:

- a) Full scale measurement of the force required to overcome the friction force of a vehicle's tyres on the roadway surface in various water depths;
- b) Knowing the full scale forces required to initiate vehicle instability, scale model testing of the hydrodynamic forces to reproduce the vehicle instability.

Full scale testing of moving flows around the subject vehicle could not be employed in this study due to the very large flows (upwards of $12 \text{ m}^3/\text{s}$) required to achieve it. Instead a number of tests were conducted by winching the test vehicle relative to a water body at various depths in a tow tank. This allowed full scale testing of buoyant friction forces under varying water levels.

Moving of the full scale vehicle to determine the vehicle instability force was achieved using a high powered winch to drag the vehicle sideways as illustrated schematically in Figure 4-1 and in practice in Figure 4-2.

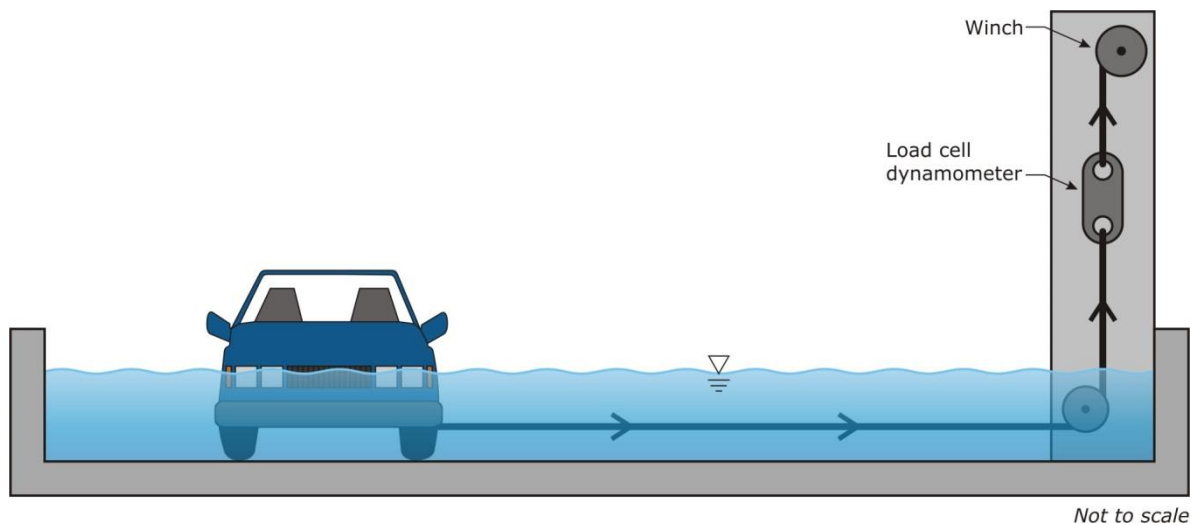


Figure 4-1: Schematic illustration of prototype scale test rig



Figure 4-2: Nissan Patrol in WRL’s wave basin facility, preparing for a winch test from the rear axle

Forces were considered separately at the vehicle front and rear axles. This allowed consideration of stability of the vehicle as a whole, or stability failure when traction is lost at one axle first and then rotated into alignment with the direction of flow. Specifically, a substantial part of the testing focused on the stability of the rear axle as floating of the rear of the vehicle has previously been identified as the most likely initiation point of instability of a vehicle exposed to floodwaters.

The choice of the axles as reference points on the vehicle provides a number of advantages. Fundamentally it allows consideration of the forces through their point of action (i.e. friction at the wheels) and particularly the separation of forces at the front and rear axles allows the measurement of the instant of traction loss at the rear axle. The axle provides a convenient location for vehicle force measurement that does not load or unload the vehicle suspension..

Scale model testing was then completed to determine the equivalent hydrodynamic forces required to reproduce the prototype scale vehicle instability forces. Further, detailed description of the experiment methodology is provided in the following sections.

4.2 Formulation of the problem

The point of loss of traction, and therefore vehicle stability, is that point at which the hydrodynamic force (F_H) applied to the vehicle overcomes the friction force (F_F) of the wheels:

$$F_H > F_F \quad (1)$$

The friction force is dependent on the downward force on the wheels, and may be considered as a vehicle as a whole, at an individual wheel, or at an axle:

$$F_F = \mu (W - B - L) \quad (2)$$

Where:

W is the weight of the vehicle;

B is the buoyancy which is dependent on the water depth (d);

L is the uplift force due to water impacting the vehicle which is dependent on the water depth and velocity; and

μ is the coefficient of friction between the tyres and the road.

Note that once the tyres are sliding, the coefficient of force (μ) decreases and it becomes more difficult for the vehicle to regain traction.

The hydrodynamic force can be expressed in the form of a drag force as:

$$F_H = 0.5 \cdot \rho \cdot A \cdot C_D \cdot v^2 \quad (3)$$

Where:

ρ is the water density;

A is the projected (profile) area of the vehicle impacted by water;

C_D is the coefficient of drag which is dependent on the water velocity and depth; and

v is the depth-averaged flow velocity.

The coefficient of drag is a complex term capturing the influence of the shape of the vehicle and the response of the flow to the obstruction. The coefficient of drag needs to be determined experimentally for each vehicle, and varies with flow depth and velocity.

Combining equations (1), (2) and (3), including the dependencies, a vehicle is stable when:

$$\mu (W - B(d) - L(d,v)) > 0.5 \cdot \rho \cdot A(d) \cdot C_D(d,v) \cdot v^2 \quad (4)$$

In determining the conditions for vehicle stability, the focus of this research is the investigation of factors that affect the friction force (μ and B), and the coefficient of drag for the vehicle. A discussion of the theoretical background and relevant knowledge on each of these parameters is provided in the following sections.

4.2.1 Friction force of a vehicle

Bonham and Hattersly (1967), after a detailed review of studies completed between 1930-1936 at the Road Research Laboratory in England (Bird et al., 1936) and consultation with Olympic Tyre and Rubber Co., arrived at a single conservative value for the coefficient of tyre friction. This was based on a braking force coefficient of 0.5 on a worst case scenario of "a smooth causeway surface on a wet country road". Adjustments were made for a reduced sideways force compared with braking force (10%), the reduced slipping force compared with peak braking

force (20%), and a further reduction due to debris that may become caught under the wheels (20%). This resulted in a friction coefficient of $\mu = 0.3$ that was used uniformly across all their tests. This value has been widely adopted in subsequent studies of vehicle stability in water, including Keller (1992) and Kramer (2016).

While this is a suitably conservative value where actual data is limited, it is worth revisiting the range of friction coefficients likely to be encountered in real world conditions. This review considers both changes in tyre and road technology and modern motoring conditions for the interpretation of measured test results.

Most available tyre traction data relates to straight line traction (braking), or cornering at speed. Limited analysis is available on the lateral grip of tyres while stationary. Rubber has a unique property whereby the force required to initially break traction is higher than the force required to maintain motion once traction is lost (Wong, 1993). In the available literature, these forces are known as *Peak* and *Sliding* forces. It is important to distinguish between these forces for vehicle stability, where it is unlikely that a vehicle will regain traction once it has been lost.

Wong (1993) provides typical coefficient of friction values for a range of conditions as reproduced in Table 4-1. This information is derived from an investigation in 1957 (Taborek, 1957), so is somewhat dated, but broadly consistent with values for modern tyres and conditions. Note that the values in Table 4-1 are for the coefficient of adhesion between rubber and concrete, rather than the braking effort coefficient. The braking effort coefficient more broadly includes the dynamics of the tyre at speed and under braking loads.

Table 4-1 Coefficient of Friction (adhesion) values between tyres and road surfaces, from Wong (1993)

Road Surface	Peak Value	Sliding Value
Asphalt and concrete (dry)	0.80 – 0.90	0.75
Asphalt (wet)	0.50 – 0.70	0.45 – 0.60
Concrete (wet)	0.80	0.70
Gravel	0.60	0.55
Earth road (dry)	0.68	0.65
Earth road (wet)	0.55	0.40 – 0.50
Snow (hard-packed)	0.20	0.15
Ice	0.10	0.07

A number of important conclusions can be drawn from this information. Significantly, concrete surfaces perform significantly better than asphalt in the wet by up to 40%. This alone is an important factor in the stability of vehicles on bridges and causeways. The presence of dirt and gravel on the roadway surface significantly decreases traction. Causeways will likely be affected during floods as mud, sand, gravel and debris are washed downstream and over the causeway. In particular, once vehicle sliding is initiated, the friction force reduces markedly (see sliding factors in Table 4-1), meaning that it is likely that the vehicle will continue to move once initial traction is lost.

There is a wealth of more recent information on tyre friction, largely targeted at vehicle accident forensics. However the focus of this traction research is on braking deceleration as an average over a distance, rather than the instantaneous peak traction, and is based on the braking effort rather than coefficient of adhesion. As such many of the quoted values are lower than those provided in Wong (1993) (see <http://www.mfes.com/friction.html> for many references).

A valid conclusion is that it is likely that the coefficient of friction from traction tests on a stationary vehicle will be somewhat higher than those of a vehicle at speed.

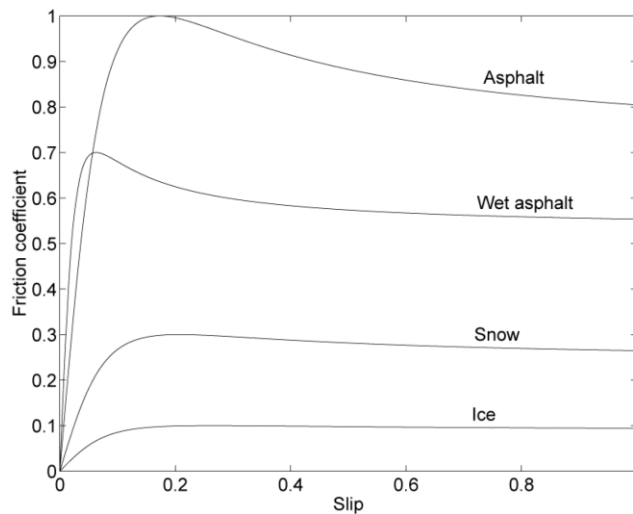


Figure 4-3: Slip curves for various road surfaces, extracted from Gerard (2006)

Figure 4-3 presents the friction slip curves from Gerard (2006). This figure demonstrates that there is a peak in the friction coefficient at low slip rates that is significantly larger than for a fully slipping tyre. The peak is exaggerated for higher friction surfaces, but almost non-existent for slippery surfaces.

In the traction tests conducted in the present investigation, the vehicle is towed at a near constant rate set by the capability of the winch, which in turn varies with the load on the winch. As the winch pulls the vehicle through the peak of the slip friction it slows down, then as the vehicle begins to move and slip increases, the speed of the winch also increases. Thus a quasi-balance is achieved on the falling part of the slip curve where load on the winch is balanced by the friction of the tyres.

4.2.2 Hydrodynamic drag on a vehicle

A detailed literature review found that there is extensive data on aerodynamic drag on vehicles travelling forwards in air. However, there is very limited data in available literature on hydrodynamic drag forces on a vehicle motoring in an open channel water flow (i.e. water with a free surface) and even less information for the specific case associated with vehicle fatalities in floods where the flows are perpendicular to the vehicle.

Early work by Hoerner (1965) provides detail on the components that contribute to the drag of a partially submerged object analogous to a vehicle in flood water. The drag on an object in a flow can be broken into two components:

1. *Profile Drag*: due to the displacement of flow around the object which is dependent on the shape and cross-sectional area of the object; and
2. *Viscous Drag (Skin Friction)*: caused by the interaction of the objects surface with the viscous fluid, which is dependent on the length of the body and surface roughness.

If the object is in an open channel flow, the surface of the water may not be steady resulting in additional drag components:

3. *Wave Drag*: due to the deformation of the water surface, i.e. the generation of a wake; and
4. *Spray Drag*: the upward jetting of water into the air at the object.

Hoerner (1965) investigated drag forces on bodies in free-surface flows in detail, and provided drag coefficients for flat plates and cylinders piercing the surface of water flow in different flow regimes (Figure 4-4 and Figure 4-5). The cylinder provided substantially less drag than a flat plate, with a peak coefficient of drag for a short flat plate of approximately 1.7. This drag coefficient is also consistent with typical drag coefficients for a flat plate with infinite length ($C_D = 1.8$).

The relative contributions of the three components of form drag for a surfacing piercing plate was summarised in Bowen et. al. (2011), see Figure 4-6. This is for the specific case where the depth of penetration into water is equal to the plate width, so the peak in C_D is expected at a Froude number $Fr=1$.

By way of background, the Froude number, Fr , is a dimensionless value that describes different flow regimes of the open channel flow encountered on floodplains. The Froude number is a ratio of inertial and gravitational forces of the flow and can be described by the equation:

$$Fr = \frac{v}{\sqrt{gD}} \quad (5)$$

Where:

- v = Depth-averaged flow velocity
- D = Hydraulic depth (cross sectional area of flow / top width)
- g = Gravity acceleration

When:

- $Fr = 1$, critical flow,
- $Fr > 1$, supercritical flow (fast rapid flow),
- $Fr < 1$, subcritical flow (slow / tranquil flow)

Hoerner's (1965) description of drag on a surface piercing object provides some important insights for this study. A significant peak in the coefficient of drag on a flat plate occurs around a Froude $Fr=1$, which may be around 50% higher than in other flow regimes. This peak moves to higher Froude numbers as the depth to width ratio of the object decreases. This may be a particularly important point of interest for the case of a vehicle passing over a bridge or causeway on a floodplain where the change in floodway flow area as is conducive to producing flood flow conditions approaching Froude $Fr = 1$ (see Figure 4-7). At the condition near Froude $Fr = 1$, the free-surface becomes undular since small changes in flow energy lead to large changes in flow depth, substantially increasing the drag on the object. This flow behaviour can also be observed anecdotally in photos and videos of flooded vehicles crossing causeways and in scale laboratory testing, with deep standing waves occurring at each end of the vehicle.

The plate scenarios tested by Hoerner (1965) are somewhat different to the case of a vehicle on a road because:

- The vehicle shape is significantly more complex including a void underneath the vehicle above the road surface;

- The width versus depth of the vehicle is outside the range of conditions covered by Hoerner; and
- There is a bottom boundary, being the road surface, that is not covered by Hoerner.

The situation of a vehicle in floodwaters is substantially more complex than the simple shapes studied by Hoerner (1965). The vehicle may be exposed to shallow water flows leading to an additional interaction with the lower (road surface) boundary. The width versus depth of the vehicle is outside the range of conditions covered by Hoerner (1965) and the vehicle itself has a complex shape, particularly with the presence of a second set of wheels behind the first, as well as a relatively rough vehicle underbody.

The additional component of skin friction underneath the vehicle is acknowledged, but has not been addressed as it is considered to be small compared to the form drag components of the vehicle.

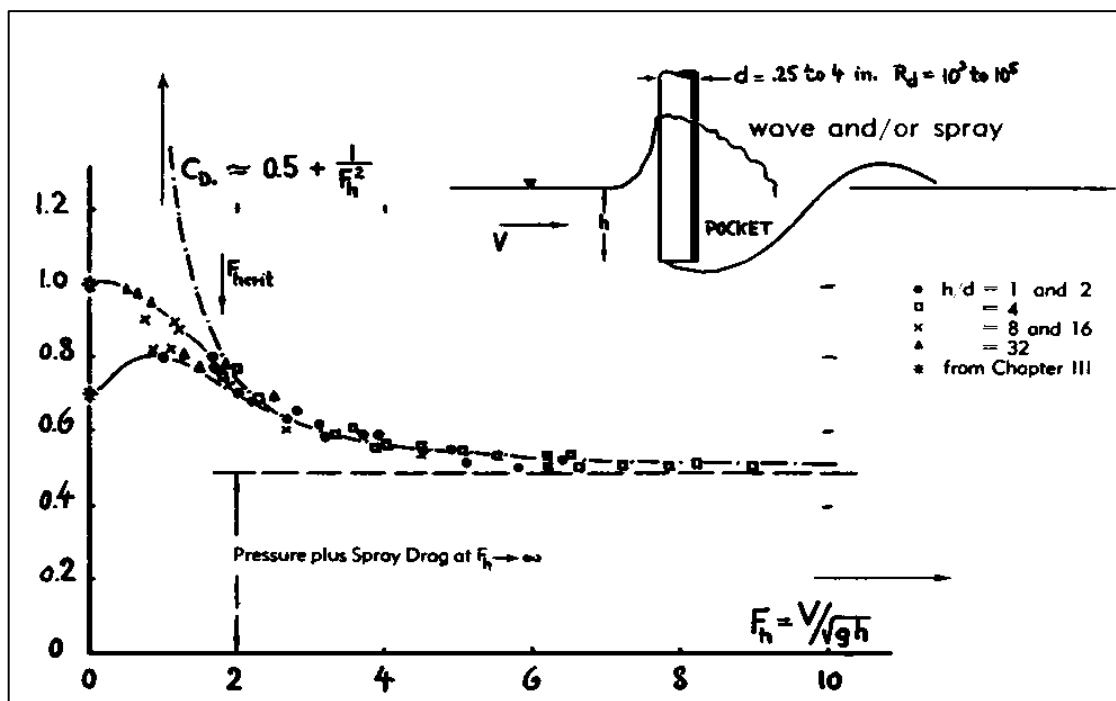


Figure 4-4 Drag coefficient of surface-piercing circular cylinders (on area d times h) as a function of Froude number, extracted from Hoerner (1965)

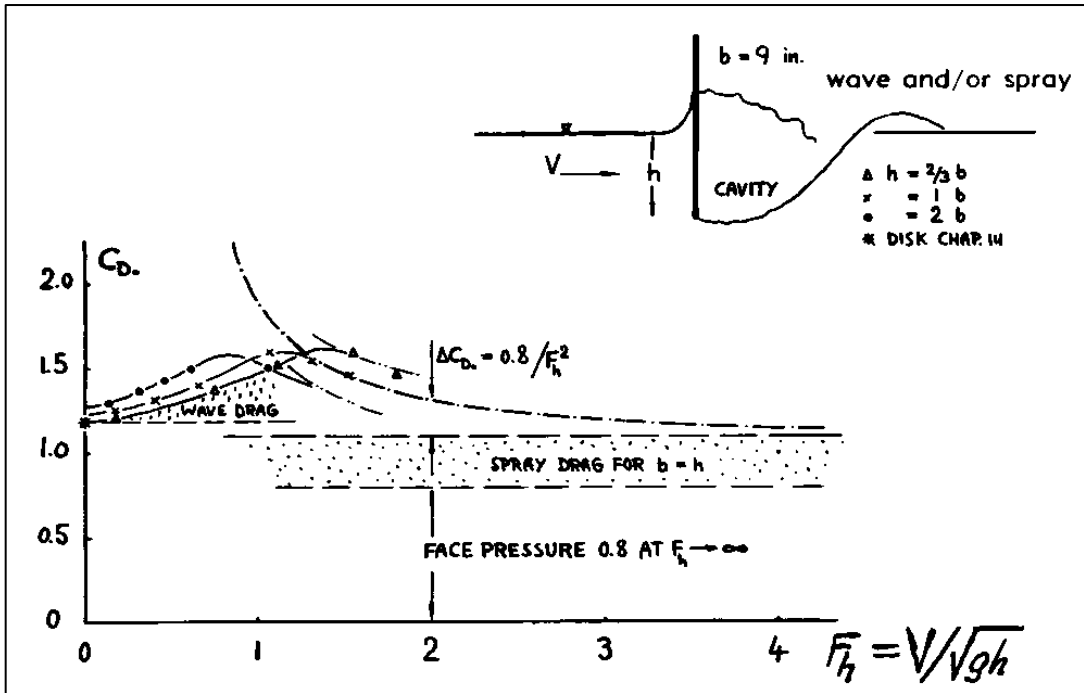


Figure 4-5 Drag coefficient of surface-piercing flat plates (on area b times h), extracted from Hoerner (1965)

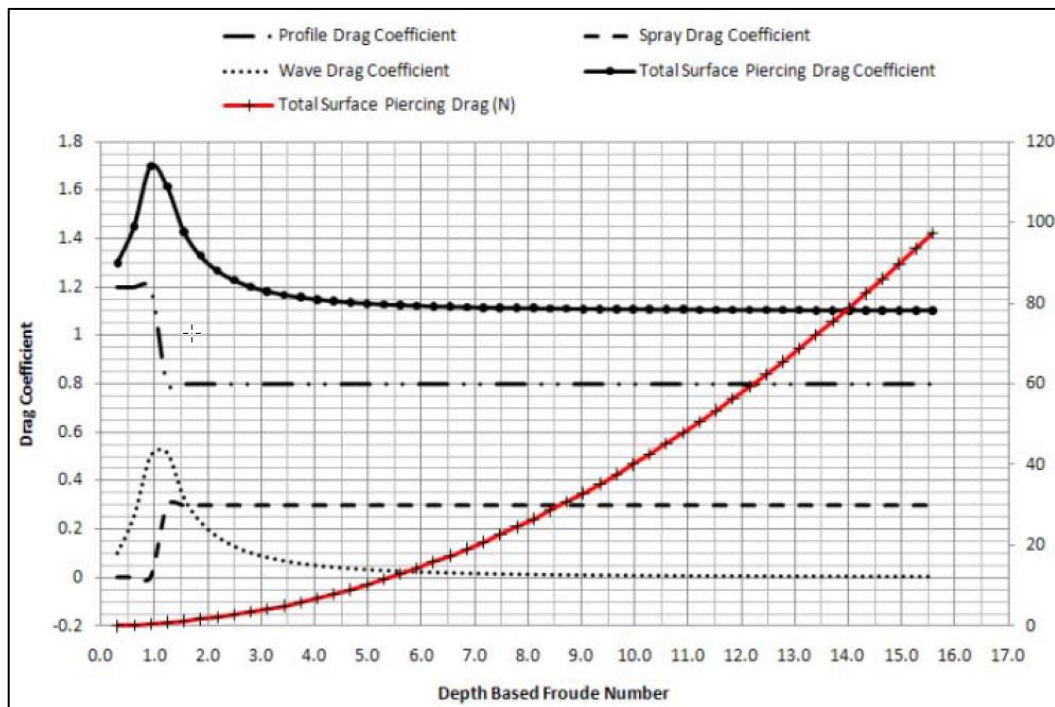


Figure 4-6: Hoerner's (1965) formulation for surfacing piercing drag, extracted from Bowen et. al. (2011)

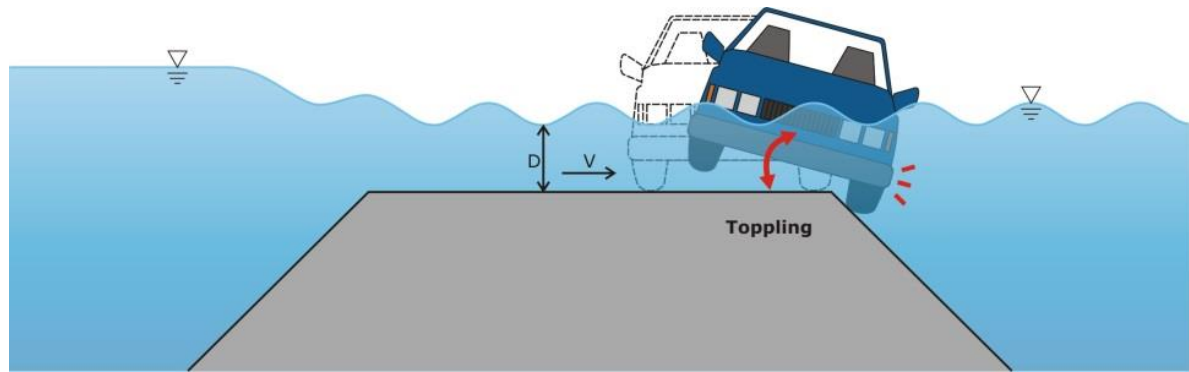


Figure 4-7: Flood flows over a causeway approaching Froude $Fr = 1$

Uplift forces

Vertical forces on the vehicle due to hydrodynamic effects are referred to here as uplift forces, though it has been observed that these may also be negative, pulling the vehicle downwards.

Discussions with the authors of Gordon and Stone (1973) suggest that uplift due to the impact of flow into a vehicle's wheel would contribute to destabilisation of the vehicle. But like horizontal drag, the processes leading to a vertical uplift force are complex. Flows impacting the upstream underbody may force the vehicle upwards. Alternatively, accelerated flows under the vehicle may act to pull the vehicle downwards. Rocking of the vehicle on its suspension would present an angled underbody to the flow. Differential water levels upstream and downstream of the vehicle lead to an uneven buoyancy. The nature and magnitude of each of these factors will vary in different flow depths, velocities and flow regimes. These aspects could not be quantified in the present study.

Variable Flow Conditions

The flows impacting a vehicle during actual flooding conditions will typically be far from steady or uniform. The flows may be turbulent and pulsating, include eddies, and vary as the flood progresses. Flows may also contain high sediment loads, affecting the floodwater's viscosity or have high debris load which will impart impact forces on the vehicle if the debris is large.

Unsteady flows will rock the vehicle from side to side, affecting both hydrodynamic forces on the vehicle (horizontal and vertical) and the instantaneous traction force available at the tyres. This is particularly pertinent to vehicle stability due to the difficulty in regaining tyre traction once it is lost.

While the additional complexity from variable flow conditions is acknowledged, this study only considered the conservative case of steady flows.

5. Full Scale Vehicle Traction Tests

5.1 Overview

The aim of the traction tests was to measure the force required to break traction at varying water depths.

The friction of the tyres against the road is directly related to the weight at the tyre-road interface and the coefficient of friction between the tyres and the road. As the water level rises, the vehicle becomes more buoyant and less vertical force is available at the tyres to maintain traction.

The testing procedure was designed to, as closely as possible, mimic the conditions of a vehicle entering a flood flow. By flooding the test tank quickly to ensure minimal water ingress into the vehicle cabin, and then towing the vehicle sideways (perpendicular to the direction of travel) using a winch assembly attached to the wheel hub, it was possible to measure the force required to break traction for the entire vehicle or specifically at the rear axle.

A rapid flood situation is typical of rising flood waters or driving into floodwaters, where the ingress of water into the vehicle is limited by the effective cabin and door seals found in modern vehicles. This situation when the vehicle is at its most buoyant, and therefore most vulnerable, is considered the worst-case scenario. A vehicle submerged for some time will be filled with water, be less buoyant and therefore require more force to move.

The winch test assembly consisted of a vertically arranged vehicle winch, a dynamometer (to measure the forces), and a pulley. This allowed the winch and instrumentation to be clear of the water during testing (see Figure 4-1).

5.2 Test vehicles

Two vehicles were tested in this study. Their selection was based predominantly on availability and the representativeness of two ends of the vehicle spectrum: a lighter modern vehicle that would be more easily swept away in flood waters (Toyota Yaris), and a typical large 4WD (Nissan Patrol). Specifications for each vehicle are provided in Table 5-1.

Table 5-1: Vehicle specifications of prototype vehicles in present study

	Toyota Yaris Sedan 2006	Nissan Patrol GRII 1998
Vehicle Weight	1045 kg	2478 kg
Length	4.3 m	4.97 m
Width	1.69 m	1.84 m
Floorpan Height (measured)	0.155 m	0.50 m
Modifications	None	Front Bull Bar, Kick Plates
Tyres	Front: Bridgestone Potenza 195/60R15 Rear: Hankook Optimo 185/60R15	Dunlop Grandtrek 265/70R16

The Toyota Yaris is representative of smaller vehicles most vulnerable to instability in floodwaters and therefore of interest for defining limits for floodplain management and

emergency planning. Characteristics such as light body weight, watertight body, and relatively low floor pan level make these types of vehicles more vulnerable to floodwaters.

Recent research by Haynes et al., (2016) noted that vehicle related flood fatalities in 4WDs have increased in the last 15 years in Australia. Testing of the Nissan Patrol 4WD provided further information for vehicles that may be more likely to be deliberately driven into floodwaters. This test case is also relevant to flood rescue vehicles, which are generally by 4WD vehicles or larger. Photographs of the test vehicles are provided in Figure 5-1 and Figure 5-2.



Figure 5-1: Toyota Yaris in WRL’s test facility, preparing for a winch test from both axles



Figure 5-2: Nissan Patrol in WRL’s wave facility, preparing for a winch test from the rear axle



Figure 5-3: Winch assembly in WRL Lab#2, including (a) framework, winch and dynamometer, (b) pulley and wheel attachment

5.3 Tyre coefficient of friction

The coefficient of friction between the concrete floor of the test facility and the vehicle tyre was tested. Testing was performed on a tyre set to specified pressure, with the vehicle winched sideways (perpendicular to the direction of motion), and wheels locked (handbrake on and automatic transmission set to "park"). The results include the effect of tyre deformation, so are somewhat different to the coefficient of friction between surfaces provided by Wong (1993), and the coefficient of friction under braking more generally tested (both discussed in Section 4.2.1).

The Toyota Yaris was tested in WRL's tow tank. The vehicle weight was estimated using the specified vehicle wet weight (1045 kg) plus the driver load of 60 kg (chosen for a small to medium sized adult). The tow force is the average of two tests conducted on the vehicle towed from both axles on a wet concrete floor.

The Nissan Patrol 4WD coefficient of friction was tested twice, on both a wet floor and dry floor. Tests of the coefficient of friction were conducted by towing the vehicle from the rear axle only. The weight of the 4WD vehicle at the rear axle was measured directly by using the dynamometer to lift the rear wheel vertically. The wheel was lifted only enough for the tyre to clear the ground, to minimise unloading of the other tyres. This approach may overestimate the vehicle weight, resulting in an underestimate of the coefficient of friction.

The results of these tests are provided in Table 5-2. A comparison between the two conditions for the Nissan Patrol is consistent with Wong (1993) which indicates that there is little difference in the coefficient of friction on wet or dry concrete.

Appropriate corrections to the traction force due to the difference between the coefficient of friction in the ideal laboratory conditions provided here and a suitably conservative coefficient of friction to be used in estimating the stability of vehicles in flood waters is discussed in detail in Section 4.2.1.

Table 5-2: Coefficient of friction results*

	Nissan Patrol	Nissan Patrol
Method	Wet Floor, Rear Axle	Dry Floor, Rear Axle
Vehicle Weight	(1290kg)	(1290kg)
Tow Force	(964kg)	(1011kg)
Coefficient of Friction μ	0.75	0.78
Conservative Coefficient of Friction μ	0.3	0.3

*Unfortunately direct measurements for coefficient of friction were not completed for the Toyota Yaris

5.4 Overview of traction tests

Traction tests were conducted on the two vehicles in varying water depths. This demonstrated the reduction in traction force required to move the vehicle as static buoyancy lifted the vehicle.

In all cases the vehicle was winched sideways (the winching cable was perpendicular to the driving direction). The cable arrangement was set so that the cable was perpendicular to the ground and no vertical loading was applied by the winch. Tyres were checked daily to ensure the specified tyre pressure was used throughout the testing program. The dynamometer was zeroed immediately prior to each test. The output from the dynamometer was logged at 5Hz for data post-processing. The accuracy of the dynamometer is 8 kg, being 0.1% of its full scale 8 tonnes, and has a measurement error of +/-2 kg.

The resulting time series of traction force as measured by the dynamometer were subsequently analysed. The peak traction reading for each test was logged and was used for the analysis of vehicle stability later in this study.

The Toyota Yaris testing was conducted for three (3) scenarios:

- With an equivalent driver occupant only of weight 60 kg (small adult), winched from the rear axle.
- With a driver occupant only of weight 60kg, winched from both axles.
- With four occupants having a combined weight of 240 kg distributed between 4 seats, winched from the rear axle.

Vehicle occupants were represented using sandbags.

The rear axle only tests provided the stability limit state as it is expected that the reduced vehicle weight over this axle will lose traction first (see discussion in Section 2). The tests on winching the whole vehicle (both axles) provided data for the calculation of the coefficient of friction, as well as validation data for assessment of the vehicle stability as a whole. To ensure the minimum amount of water ingress into the Toyota Yaris, the basin was rapidly filled in less than two minutes from an adjacent reservoir basin using a flood gate (Figure 5-4).



Figure 5-4: Rapid filling of WRL's test tank (wave basin). The winch assembly is also shown.

The Nissan Patrol 4WD, was tested in two (2) WRL facilities. Initial tests in the first facility (wave basin) provided water depths up to 660 mm. Subsequent modelling in the second facility provided deeper water conditions (of up to 1.3 m) which enabled the 4WD vehicle to float with the rear wheels lifted off the ground. All 4WD testing was conducted with loading for a single driver occupant (60kg), and was winched from the rear axle only.

Due to the slower fill time of the second laboratory facility (Lab 2), accessible leakage points in the 4WD cabin were sealed with silicon, and a submersible pump was used to evacuate water ingress. In this way the vehicle would remain buoyant for an indefinite period, even at high water levels.

For both test methods, there was some small pooling of water towards the front of the vehicle cabin, estimated to be less than 50L in both cases. Pooling in the floor of the cabin was always at the front of the vehicle because the higher rate of buoyancy at the rear of the vehicle tilted the vehicle forwards. This filling would increase the resulting measured traction force somewhat. However, it is considered negligible because the majority of the effect would be at the front wheels, while the rear is the critical point of vehicle instability. Some ingress of water would be anticipated into vehicles in real world flood emergencies in all but the most extreme rapid submersion scenarios (e.g. driving at speed into rapidly deepening waters).



Figure 5-5: Toyota Yaris in WRL's wave basin facility, in 0.6 m water depth with rear wheels clear of the floor



Figure 5-6 The lead author demonstrating zero traction at the rear wheels for the Nissan Patrol 4WD in WRL's Lab#2 testing tank. Water depth is approximately 1.0m.

5.5 Test results

Time series of traction force for each test is provided in Figure 5-7 to Figure 5-9 for the Toyota Yaris, and Figure 5-10 for the Nissan Patrol 4WD. Note that the forces have been converted to kN for these figures, while the data recorded by the dynamometer is in metric tonnes.

Results of the peak measured traction force (the maximum force measured) for tests on the three (3) cases for the Toyota Yaris are provided in Table 5-3. Results of the peak measured traction force for tests on the Nissan Patrol 4WD are provided in Table 5-4.

Points on the vertical axis (traction force $\approx 0\text{kN}$) indicate those depths where the vehicle could be pushed by hand. In these tests, the vehicle floated while a constant hand pressure applied by an observer. The instant at which the vehicle would move sideways, the water level was recorded. In all cases the rear wheels would rise off the ground while the front wheels remained grounded. Pushing the side of the vehicle towards the rear would pivot the vehicle around the front wheels.

Measurement Uncertainty

The accuracy of the dynamometer is 0.1% of full deflection (8kg or 78.48N). Other sources of error, such as pulley friction, are estimated to be less than 100N. Error in the measurement of water depth is largely due to water level fluctuations following rapid filling and are estimated to be less than 20 mm.

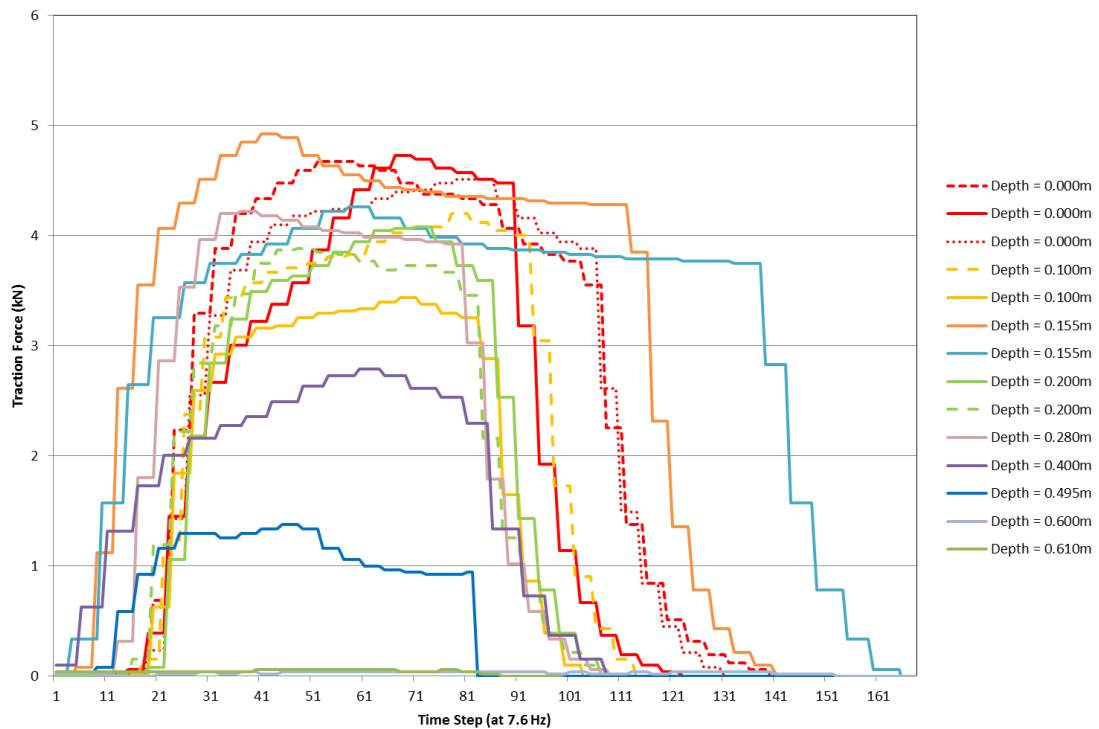


Figure 5-7: Traction force time series for tests on the Toyota Yaris with one driver occupant, winched from the rear axle only

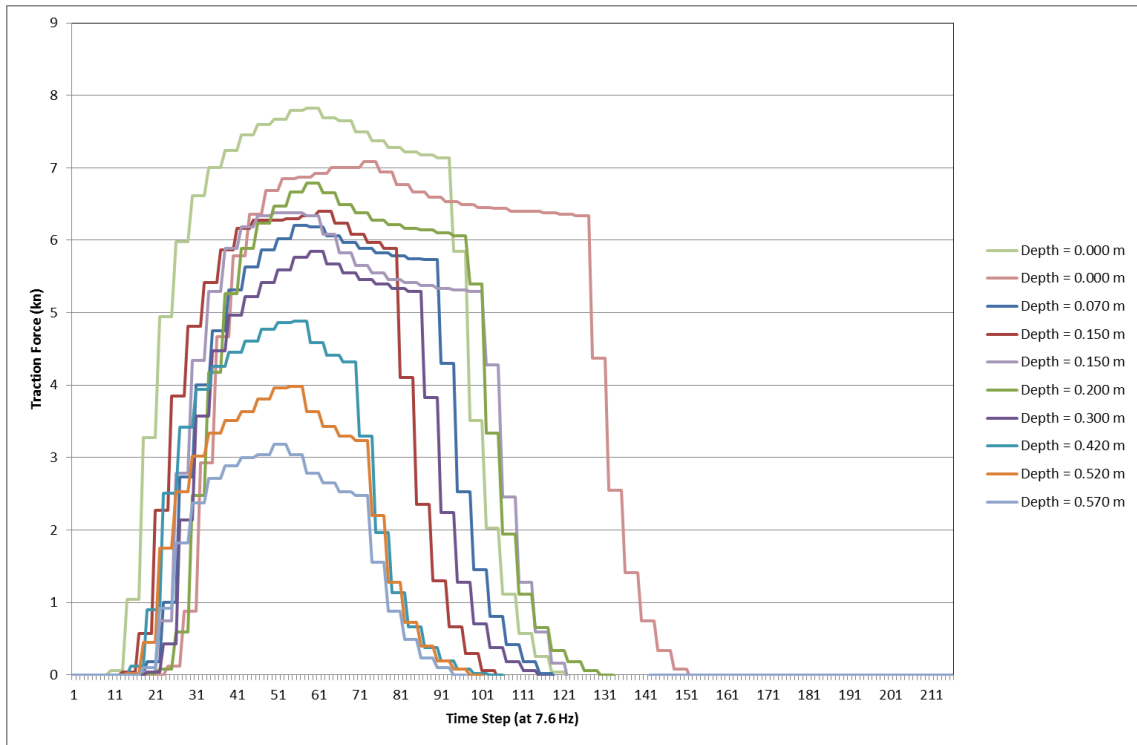


Figure 5-8: Traction force time series for tests on the Toyota Yaris with four occupants, winched from the rear axle only

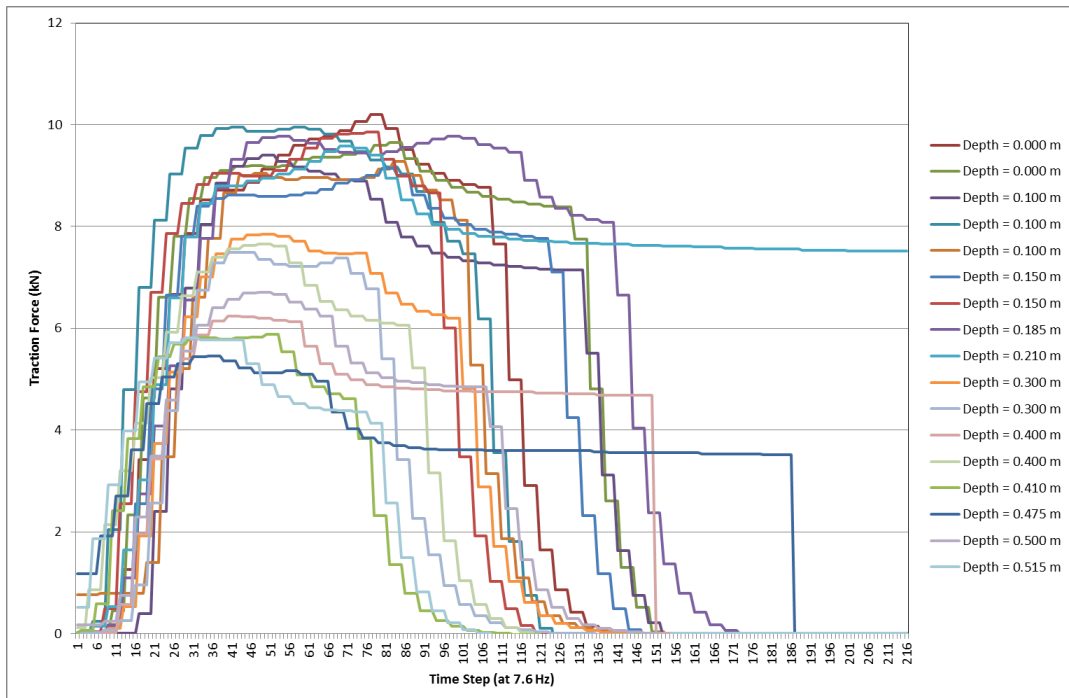


Figure 5-9: Traction force time series for tests on the Toyota Yaris with one driver occupant, winched from both axles

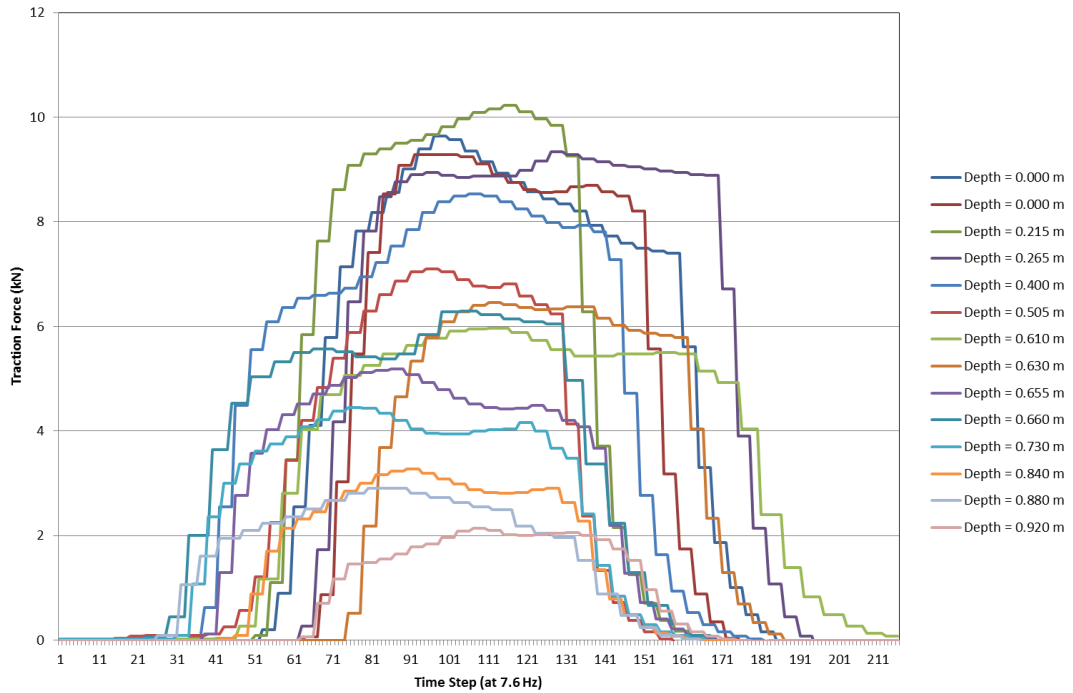


Figure 5-10 Traction force time series for tests on the Nissan Patrol with one driver occupant, winched from the rear axle

Table 5-3: Measured peak horizontal traction force results for the Toyota Yaris

One Occupant, Rear Axle		One Occupant, Both Axles		Four Occupants, Rear Axle	
Water Depth (m) D	Horizontal Force (kN)	Water Depth D (m)	Horizontal Force (kN)	Water Depth D (m)	Horizontal Force (kN)
0.00	4.670	0.00	10.202	0.00	7.083
0.00	4.728	0.00	9.653	0.00	7.828
0.00	4.513	0.10	9.398	0.07	6.200
0.10	4.199	0.10	9.947	0.15	6.396
0.16	4.258	0.10	9.280	0.15	6.377
0.16	4.925	0.15	9.143	0.20	6.789
0.19	4.081	0.15	9.849	0.30	5.847
0.20	3.885	0.19	7.770	0.42	4.885
0.25	3.983	0.21	9.575	0.52	3.983
0.28	4.218	0.30	7.848	0.57	3.178
0.35	4.042	0.30	7.495		
0.40	2.786	0.40	6.239		
0.49	1.373	0.40	7.652		
0.50	2.021	0.41	5.886		
0.56	0.000	0.48	5.454		
0.60	0.000	0.50	6.710		
0.61	0.000	0.52	5.808		

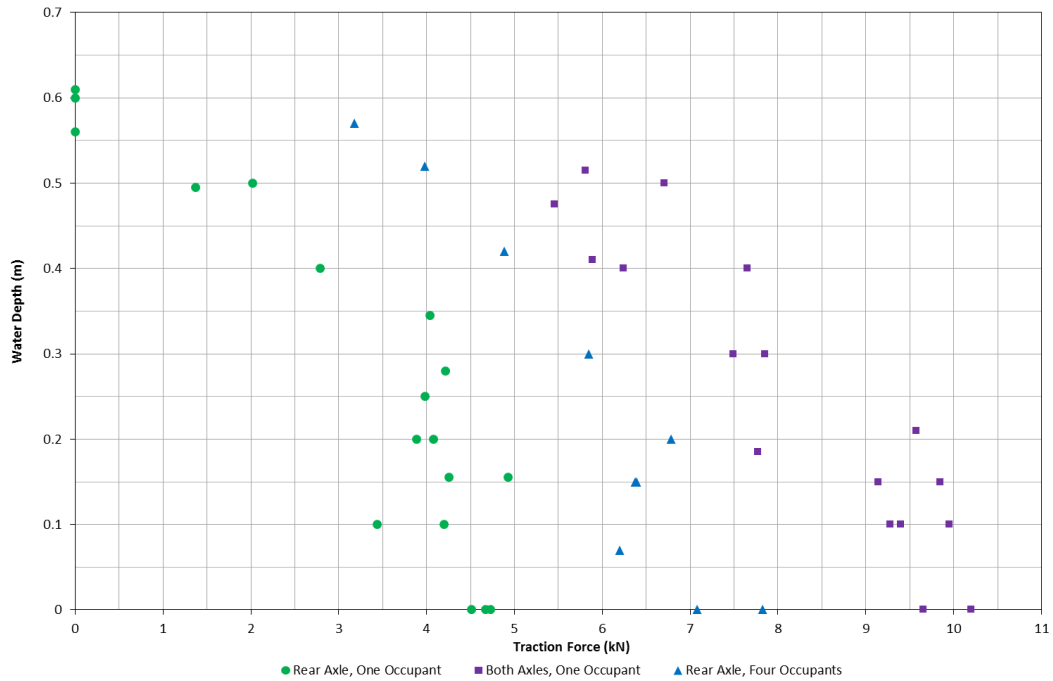


Figure 5-11: Measured peak horizontal traction force for a Toyota Yaris 2006 in varying static water levels. Tests were conducted on three scenarios with varying passenger loads and tow points

Two passenger scenarios i) driver only; and ii) driver plus three (3) passengers were tested in the Toyota Yaris. These results showed that the number of passengers in the car affected the vehicle stability threshold and that the limiting case was the case with the driver only. The additional passengers increased the overall vehicle weight resulting in an increase in the traction force. Tests were also conducted to determine the difference between the threshold force to move sideways by pulling both front and rear axles and the rear axle only. Test results noted that, as is observed in video footage of real flood situations, the limiting case is the case of rear axle instability where the rear (no engine) end of the car floats first causing the car to pivot on the front wheels and roll in the direction of flow. Since the limiting case was shown to be rear axle instability, further testing of the Nissan Patrol 4WD was for the rear axle only.

Table 5-4: Measured peak horizontal traction force results for the Nissan Patrol

One Occupant, Rear Axle	
Water Depth D (m)	Horizontal Force (kN)
0	9.633
0	9.280
0.265	9.339
0.4	8.535
0.505	7.102
0.61	5.964
0.63	6.455
0.655	5.180
0.66	6.298
0.73	4.455
0.84	3.277
0.88	2.903
0.92	2.139
0.97	0.000
0.98	0.000

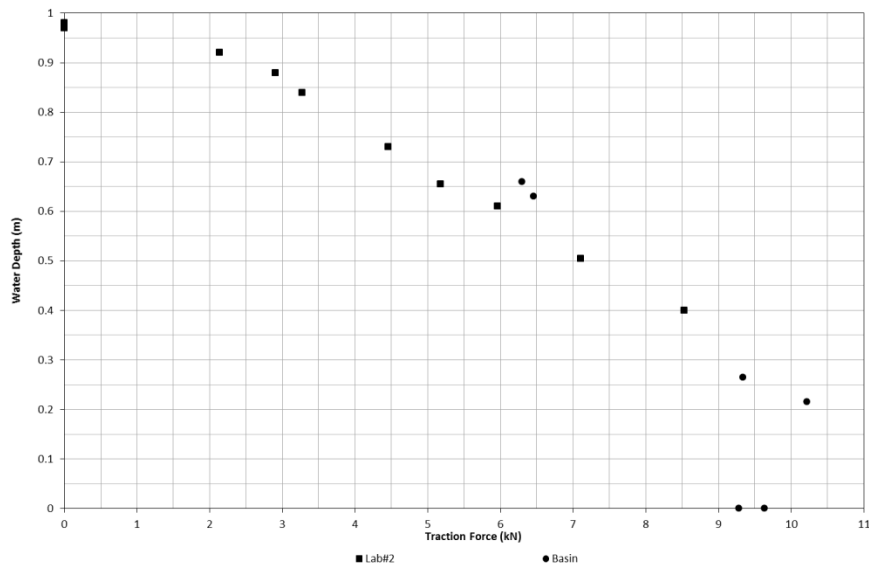


Figure 5-12: Measured peak horizontal traction force for a Nissan Patrol 4WD 1998, winched from the rear axle only, with one occupant

6. Hydrodynamic Force Testing (1:18 Scale)

6.1 Overview

Hydrodynamic force testing was conducted on a scale model vehicle to determine the coefficient of drag (C_D) for the vehicle by direct measurement of hydrodynamic drag forces on the vehicle. The tested flows were typical of those capable of destabilising a vehicle and ranged from subcritical ($Fr = 0.3$) to supercritical ($Fr = 4.2$) flows. The resulting coefficient of drag determined in the testing was used in Equation (4) to develop the stability curves presented in Section 7.

Hydrodynamic testing was conducted in a 1 m wide tilting flume. The flume was a rectangular channel with a parabolic entrance condition providing smooth and calm inflows. The tail water condition could be controlled with a hinged gate at the tail of the flume. In all tests the flume was kept horizontal to ensure the horizontal force component was accurately measured.

The model scale was chosen to suit available diecast model vehicles. A scale of 1:18 is commonly used for scale cars and provides very good replication of body dimensions and detail, including underbody roughness. Unfortunately a model identical to the vehicle used in the winch tests could not be sourced. Instead a Toyota Yaris 2005 Hatch (rather than a sedan) was used in the testing. This provided similar body features, curvature and underbody roughness, though the overall body length was different.

Model scaling was based on geometric similarity with an undistorted length scale of 1:18 used for all tests. The scaling relationship between length and time was determined by Froude similitude, with the following relevant scale ratios (prototype divided by model) being adopted for the model:

- Length ratio $L_R = 18$
- Time ratio $T_R = L_R^{0.5} = 4.243$
- Velocity ratio $V_R = L_R^{0.5} = 4.243$
- Discharge ratio $Q_R = L_R^{2.5} = 1374.62$
- Force ratio $F_R = L_R^3 = 5832$

The model vehicle was suspended by fine wire cables to a rigid frame and an adjustment mechanism that allowed the vehicle tyres to be held just above the surface of the flume. The cables were attached to each of the four wheels. The vehicle was oriented so that the flow was directly perpendicular to the vehicle (90 degrees to the direction of vehicle travel).

The weight of the model was such that the vehicle was never buoyant under any flow condition, so that only the hydrodynamic forces were measured. Buoyancy, friction and other forces were not measured in the model. The vehicle was held at a fixed level, such that loading and unloading of the springs due to buoyancy or rolling of the vehicle from side impact forces was not considered.

For the horizontal hydrodynamic force tests, fine wire cables were attached between the upstream side wheels (front and rear) and load cells mounted on a rigid frame upstream of the vehicle, see Figure 6-1. The load cells both constrained the vehicle in the longitudinal direction, as well as measuring the horizontal hydrodynamic forces on the vehicle. Forces were logged at 20Hz.

The impact on the calculation of the coefficient of drag using a scale model sedan rather than a hatch body type, is considered to be negligible as the form of the two body shapes is similar (curves at the front and rear of the vehicle) and the difference in cross-sectional area is accounted for in the coefficient of drag calculation.



Figure 6-1: Test assembly for testing of the horizontal hydrodynamic forces. Flow is from the left of the picture

Instrumentation

Forces in the model were measured using Futek LSB210 submersible load cells with full scale range of 10 Lbs (4.536 kg). A coupled amplifier was used, and sampled at 20 Hz with a National Instruments acquisition card () and LabVIEW.

Flow rates were measured using an electromagnetic flow meter with pipe diameter 100 mm. Flow depths were measured using a point gauge.

6.2 Subcritical flows (tailwater controlled)

Subcritical flows are commonly found in flood conditions. They are typically deeper, slower moving waters as demonstrated in Figure 6-2. For the experimental test under subcritical flow conditions, the Froude number range was $0.30 < Fr < 0.76$.

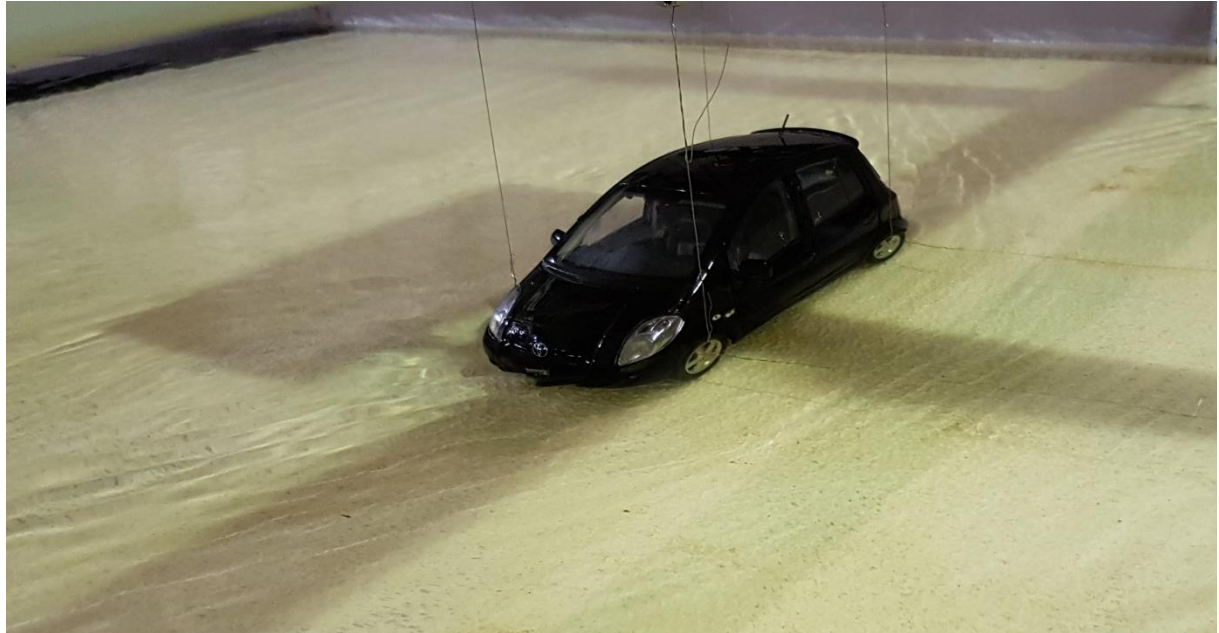


Figure 6-2: Testing of the model in subcritical flows: $Fr = 0.3$, $d = 0.71\text{m}$, $v = 0.80\text{m/s}$ (prototype)

6.3 Critical flows (broad crested weir)

Critical flows are less commonly found in floodwaters than subcritical flows, but these conditions could be approached on broad crested weir-like structures such as bridges and causeways (see Section 4). Since these floodplain structures are often used by vehicles to cross waterways, there is a reasonable likelihood that vehicles crossing floodwaters might be exposed to undular and wavy flows with near-critical flow conditions ($Fr \approx 1$).

The model was tested by suspending the vehicle and test rig over a broad-crested weir. The weir was constructed using a single sheet of plywood, approximately 19 mm thick, on the bed of the flume (Figure 6-3). No tail water control was used in these tests as flow over a broad crested weir is designed to transition the flows from subcritical flows upstream of the crest to supercritical flow downstream (i.e. the broad-crested weir acts as a flow control).

Note that it is difficult to determine the exact Froude number in these conditions. The flow over the weir is undulating, so that the Froude number varies above and below unity with distance. Since the width of the vehicle covers some distance it also covers a range of Froude numbers.



Figure 6-3 Testing of the model on a broad crested weir

6.4 Supercritical flow (undershot gate)

Supercritical flows (shallow fast flows) occur less commonly in natural systems however they may be encountered at bridges or road embankments where the water transitions through critical flow depth. Supercritical flow may also be found in urban environments where steep slopes could exist. Under flash flood conditions, steeper roadways in the upper parts of a catchment are often the predominant pathway for overland flows moving down the catchment towards pit and pipe stormwater systems and creek channels. During smaller storms, these kerb and gutter type flows would typically be well below the floor pan level of most vehicles and safely trafficable. However, in larger storms when these flows become deeper and above the floor level of exposed vehicles, the fast and turbulent nature of the flood waters may have the force to push a vehicle sideways and make it unstable.

Supercritical flows were developed in the scale test facility using an undershot gate as presented in Figure 6-4.



Figure 6-4: Testing of the model in supercritical flows $d = 0.225\text{m}$, $v=4.0\text{m/s}$ (prototype), $C_D = 1.86$, $Fr = 2.66$

6.5 Horizontal force testing results

Horizontal force test results are summarised in Table 6-1. The drag coefficient results are plotted against Froude number Fr in Figure 6-5.

Coefficient of Drag

Testing showed a range in the coefficient of drag across all flow regimes from 1.0 to 1.8. Values in the subcritical range were quite scattered, but showed a slight trend upwards over the range of Froude number from 0.30 to 0.76.

Critical flows through the tested range of supercritical flows (up to $Fr = 4.2$), showed a smaller range of coefficient of drag of 1.1 to 1.6. However, the lower values were measured in tests where the flow depths were lower than the body of the vehicle, so impact is predominantly with the wheels alone. Flows which impacted the body of the vehicle typically ranged from C_D of 1.4 to 1.6.

Table 6-1: Summary of Horizontal Force Testing (prototype)

	Test	Force Rear (kN)	Force All (kN)	Depth (m)	Velocity (m/s)	C_D	Fr
Subcritical	1	0.315	0.589	0.378	1.01	1.08	0.53
	2	0.251	0.461	0.468	0.82	0.98	0.38
	3	0.490	0.927	0.630	0.90	1.14	0.36
	4	0.437	0.781	0.711	0.80	1.06	0.30
	5	0.805	1.639	0.828	0.97	1.26	0.34
	6	0.787	1.685	0.783	1.03	1.24	0.37
	7	1.312	2.869	0.585	1.37	1.65	0.57
	8	1.283	2.770	0.585	1.37	1.60	0.57
	9	1.872	3.983	0.666	1.44	1.80	0.56

	Test	Force Rear (kN)	Force All (kN)	Depth (m)	Velocity (m/s)	C _D	Fr
	10	1.481	3.068	0.738	1.30	1.50	0.48
	11	1.359	2.747	0.801	1.20	1.44	0.43
	12	1.551	3.278	0.522	1.53	1.74	0.68
	13	0.601	1.155	0.342	1.39	1.30	0.76
	14	0.752	1.452	0.396	1.41	1.29	0.72
	15	0.869	1.703	0.414	1.44	1.37	0.72
	16	0.986	1.930	0.432	1.45	1.45	0.71
	17	1.073	2.129	0.441	1.46	1.54	0.70
	18	0.618	1.283	0.432	1.28	1.25	0.62
	19	0.717	1.475	0.459	1.27	1.35	0.60
	20	0.805	1.645	0.477	1.28	1.39	0.59
	21	0.601	1.248	0.585	1.05	1.24	0.44
	22	0.595	1.225	0.558	1.01	1.37	0.43
	23	0.443	0.921	0.531	0.98	1.17	0.43
Critical	1	1.166	2.414	0.360	1.91	1.33	1.02
	2	1.400	2.933	0.378	2.02	1.35	1.05
	3	1.849	3.972	0.450	1.97	1.53	0.94
	4	1.563	3.359	0.405	2.00	1.44	1.01
Supercritical	1	17.642	35.704	0.513	6.56	1.06	2.93
	2	10.626	22.138	0.369	5.41	1.47	2.85
	3	15.373	32.420	0.369	6.82	1.36	3.59
	4	10.509	22.039	0.378	5.26	1.50	2.73
	5	12.580	26.384	0.378	5.89	1.43	3.06
	6	9.127	19.286	0.378	4.92	1.50	2.56
	7	6.678	14.201	0.306	4.88	1.51	2.82
	8	8.946	18.569	0.306	5.80	1.39	3.35
	9	12.160	25.066	0.306	6.63	1.44	3.83
	10	2.747	5.797	0.225	3.98	1.51	2.68
	11	4.170	8.561	0.225	4.69	1.60	3.16
	12	6.374	13.046	0.225	5.75	1.62	3.87
	13	0.980	2.030	0.225	2.72	1.13	1.83
	14	1.849	3.785	0.225	3.30	1.43	2.22
	15	3.202	6.713	0.225	4.29	1.50	2.89
	16	1.930	3.750	0.225	3.16	1.54	2.13
	17	2.741	5.768	0.225	3.95	1.52	2.66
	18	0.496	0.974	0.144	2.82	1.16	2.37
	19	0.723	1.452	0.144	3.45	1.15	2.91
	20	1.067	2.123	0.144	4.20	1.14	3.53
	21	1.697	3.307	0.144	4.94	1.28	4.16

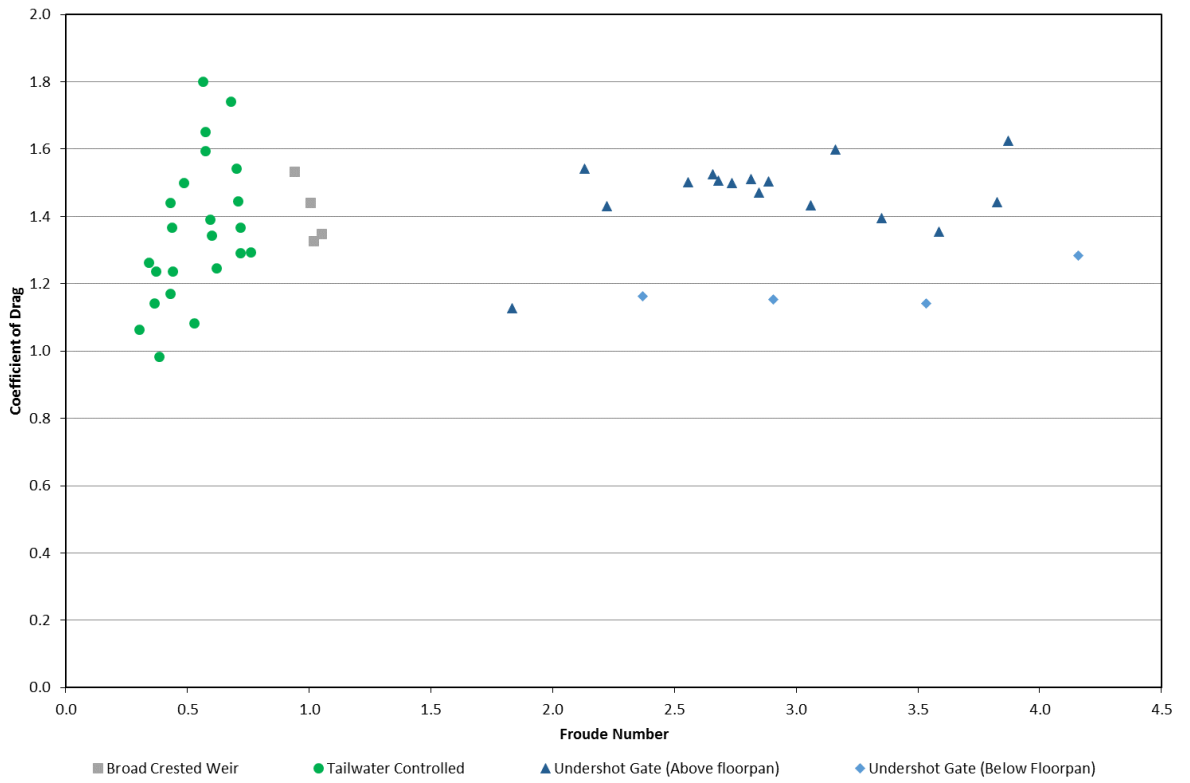


Figure 6-5 Coefficient of Drag for a Toyota Yaris based on the horizontal hydrodynamic force tests

7. Discussion of Results

7.1 Observations

This research investigation has produced two sets of results that can be considered both separately and in combination.

Prototype scale vehicle instability force measurement

Firstly, the full scale vehicle testing produced a range of test results that measured the force required for a vehicle to lose traction and become unstable for a range of water depths. Figure 7-1 plots these force thresholds for the case of rear wheel instability for the Toyota Yaris, representative of small vehicles, and the Nissan Patrol representative of larger 4WD vehicles.

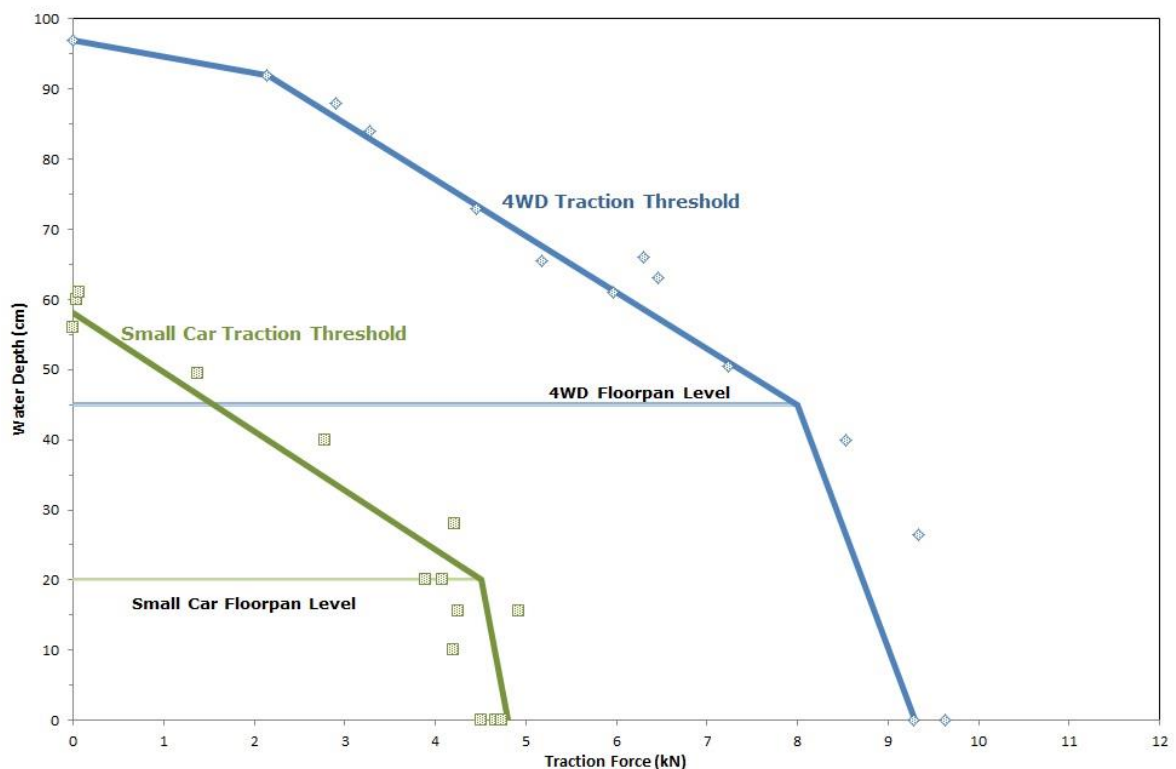


Figure 7-1: Vehicle stability deduced from prototype scale measurements – rear wheel horizontal force thresholds versus water depth

A salient observation from these test results is the clear distinction between the stability of the vehicles when the water level is below the vehicle's floor pan and once it reaches a point just above the floor pan. The buoyancy force of the air trapped in the vehicle cabin is analogous to a bubble floating on the water surface. The results in Figure 7-1 show that as soon as floodwaters are deeper than the floor of the vehicle and begin to engage with the air trapped in the vehicle cabin, the force required to move the vehicle sideways rapidly decreases. For the Toyota Yaris, this threshold depth for force reduction is approximately 0.2 m. As the flood water depth increases above 0.2 m, the force required to move the Toyota Yaris sideways rapidly decreases until the rear wheels are floating off the ground and effectively zero force is required to move the car sideways at a depth of 0.6m.

Similarly for the Nissan Patrol 4WD, at a depth of approximately 0.45 m, just above the floor pan, the force to move the vehicle sideways is markedly reduced. This force required to move the car sideways reduces rapidly until the rear wheels of the vehicle are completely off the ground, and zero force is effectively required to move the car sideways, at a water depth of approximately 0.95 m.

Model scale hydrodynamic testing

The second set of tests conducted for this research considered the hydrodynamics of flood flows impacting on a vehicle exposed to floodwaters at model scale. While numerous previous studies have considered vehicle stability at model scale, the present scale model testing had the benefit of the knowledge of the prototype flow force thresholds required for initiation of movement of the vehicles at prototype scale. Scaling of these forces to model scale enabled informed model design and testing. Model testing focussed on a range of combinations of flow depth and velocity to reproduce the scaled prototype forces. By way of further explanation, the analysis used the equations documented in Section 4.2 to guide the analysis.

Recall that a vehicle becomes unstable when the hydrodynamic force (F_H) of the incident floodwaters overcomes the friction force (F_F) (reduced by vehicle buoyancy) i.e.:

$$F_H > F_F \quad \text{(Eqn (1) Section 4.2)}$$

Since F_F has been measured in the prototype vehicle testing and the flow depth and velocity have been measured in the hydrodynamic scale model testing, the unknown parameter in the hydrodynamic force equation the coefficient of drag (C_D) can be estimated. Recalling that, the hydrodynamics force can be expressed as:

$$F_H = 0.5 \cdot \rho \cdot A \cdot C_D \cdot v^2 \quad \text{(Eqn (3) Section 4.2)}$$

A comparison of the hydrodynamic model results and the prototype test results in Figure 7-2 shows that the hydrodynamic testing reproduced a range of scaled force results that encompassed the prototype stability force testing.

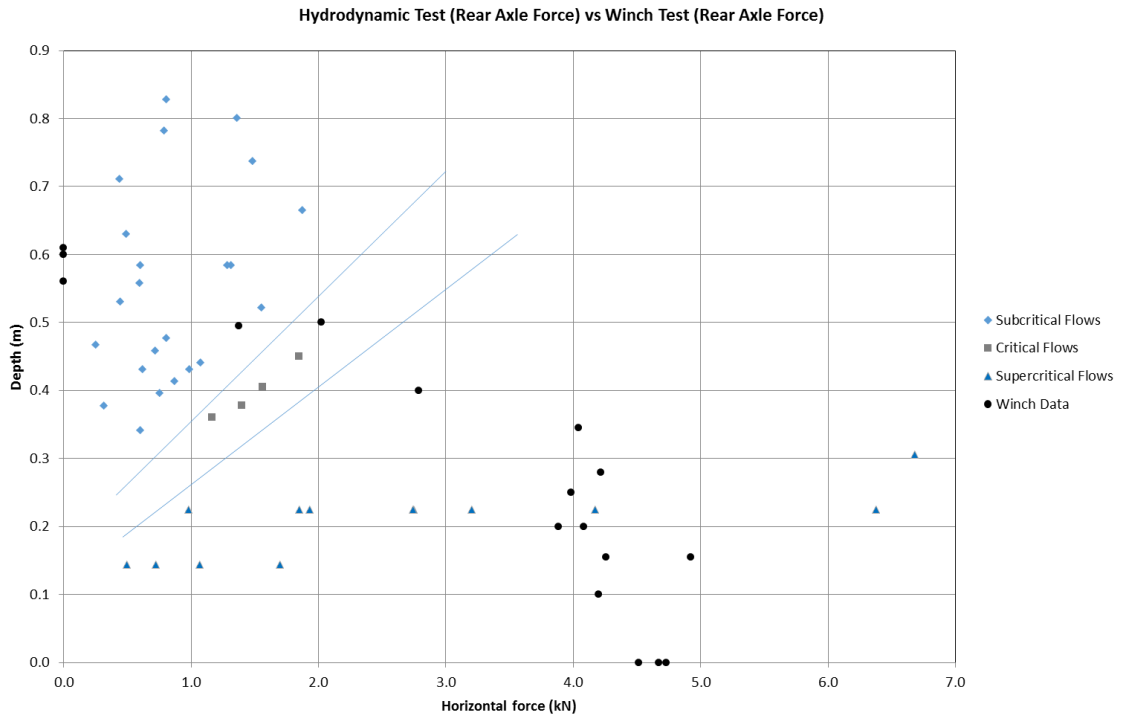


Figure 7-2: Comparison of the Force vs Depth relationship for the Hydrodynamic Tests and the Winch Tests; Toyota Yaris

The hydrodynamic testing also provided interesting results and observations on flow dynamics as the flood depth rises relative to the vehicle. It was observed that the hydrodynamic force on a vehicle rapidly rises when the flow depth meets the vehicle floor as drag is felt not only at the four wheels but across the whole side and undercarriage of the vehicle. At the same time as the flow depth interacts with the floor of the car, the stabilising weight of the vehicle begins to reduce the downward force on the tyres, and subsequently the traction available at the wheels, as the vehicle becomes buoyant. Additionally, it is likely that some hydrodynamic uplift may be felt on the upstream side of the vehicle due to the impact of water against the lower parts of the car body. All these hydrodynamic phenomena confirm the significant reduction in vehicle stability as flow depths meet the vehicle floor pan.

7.2 Comparison of tested vehicles to other vehicles

This study was conducted on two vehicles, representing a smaller, lightweight vehicle and a heavier 4WD. To gain some further insight on what might be the limiting flow conditions for lightweight vehicles, the characteristics of a range of smaller, lighter vehicles available in Australia was compiled and compared. The weight and dimensions of a number of lightweight vehicles is provided in Table 7-1.

The information compiled in Table 7-1 demonstrates that there are a number of vehicles that are lower, lighter and/or longer than the Toyota Yaris test vehicle, and so will be more vulnerable in floods. As noted earlier, a significant factor for vehicle stability is the buoyant volume of air in the vehicle cabin compared with the weight of the vehicle. Along with a trend towards lighter bodies, contemporary passenger vehicles tend to have more spacious cabins, integration of chassis and body components, and smaller engine bays. This is most notable in hatch body vehicles, where the cabin extends to the car boot, and the engine bay is minimised. Similarly,

vehicles with long sections of body and boot rearward of the rear wheels, such as wagons, will have a very buoyant rear and large aft area for flood water to impact, increasing the hydrodynamic force at the rear axle. Lower vehicles will clearly be susceptible at shallower water depths.

Vehicle body dimension limits in Australia are set by the Roads and Maritime Services (*Vehicle Standards Information No. 5*, 2012). This limits vehicle body clearance to 100 mm minimum. This is significantly lower than the vehicles tested in this study. After market modifications to small vehicles often include lowering the vehicle and this is likely to further reduce the stability of these vehicles compared to the Toyota Yaris as tested.

Table 7-1 Comparison of smaller sized vehicle weights and dimensions

Vehicle	Type	Year	Weight - Kerb (T)	Length (m)	Clearance (mm)
Toyota Yaris	Sedan	2006	1.045	4.3	155
Fiat 500	Hatch	2013	1.072	3.545	104
Ford Fiesta	Hatch	2016	1.014	4.056	155
Holden Barina	Hatch	2016	1.235	4.399	149
Hyundai i30	Hatch	2016	1.260	4.3	140
Kia Picanto	Hatch	2016	0.994	3.595	142
Lotus Elise	Convertible	2016	0.870	3.785	130
Mazda 2	Sedan	2016	1.035	4.32	150
Mazda 3	Sedan	2016	1.258	4.58	155
Mazda MX-5 Miata Club	Hatch	2016	1.124	3.995	117
Mini cooper	Hatch	2015	1.182	3.838	125
Mitsubishi mirage	Hatch	2016	0.890	3.795	160
Nissan Leaf	Hatch	2016	1.477	4.445	160
Nissan Versa	Sedan	2016	1.084	4.455	155
Peugeot 208	Hatch	2016	1.070	3.973	119
Scion IQ	Hatch	2016	1.005	2.985	135
Subaru Impreza	Sedan	2016	1.340	4.585	145
Suzuki swift	Hatch	2016	1.050	3.85	140
Toyota Yaris	Sedan	2010	1.030	4.3	117

Vehicles with rear mounted engines will have a similar response to forward mounted engine vehicles, except that the front wheels will lose traction first. Travelling into deepening waters in a rear engine mounted vehicle with the vulnerable front wheels first, means that the vehicle may well be destabilised earlier and therefore be more vulnerable than a vehicle with a front mounted engine.

The Nissan Patrol 4WD as tested can be considered representative of larger 4WD vehicles. There is a trend to 'soft' 4WD vehicles and sport utility vehicles (SUV's) that may be capable of light off-road activities, but will be substantially more vulnerable in floodwaters than the results for the testing the Nissan Patrol would indicate since these vehicles have less mass and are comparatively lower to the ground.

7.3 Testing uncertainties

The following uncertainties in the model testing are noted:

- Measurement uncertainty at both prototype and model scale. This is a minor and quantifiable uncertainty, but nevertheless present.
- Scaling effects. While the scale adopted for the modelling (1:18) was suitable for the major forces of gravity and inertia, minor forces acting on the vehicle may not be well represented at this scale;
 - The impact of very turbulent, pulsating or varying flows has not been considered but is important in initially destabilising a vehicle;
 - The changes to vehicle height and roll angle (loading and/or unloading of the suspension) due to buoyancy and side impact forces were not considered in the hydrodynamic tests;
 - The testing was conducted in ideal conditions, with regular channel dimensions and steady flows. This is rarely the case in real world conditions;
 - Uplift forces on the vehicle were poorly determined in the testing, this is largely due to the magnitude of surface tension forces compared to the weight of the vehicle. In other words, when considering the vertical forces, the weight of the water raised by surface tension was significant compared with the uplift forces. A larger scale and careful handling of this is required.
- The Coefficient of Friction between tyre and road surface in actual flood conditions, as opposed to wet road testing, is not well understood.
- Only two vehicles were tested and they do not represent the limiting case for vehicle stability.

These uncertainties are largely unquantifiable and so a level of conservatism is required when interpreting and applying the test data in this report.

7.4 Interpretation of test information for floodplain management and emergency management

7.4.1 Preamble

The prototype scale testing of vehicles conducted for this investigation has provided some stark information on the vulnerability of vehicles as they interact with floodwaters.

Testing showed that the stabilising force due to the weight of a vehicle begins to rapidly reduce once floodwaters rise above the floor of the vehicle and the 'bubble' of air contained in the vehicle's cabin imparts an uplifting buoyancy force on the vehicle. Test results showed that when flow depths increase to moderate levels, even large, heavy vehicles will reach a limiting depth where they completely float. In the testing conducted for this investigation, a large **Nissan Patrol 4WD** with a kerb weight of greater than 2.4 tonne was shown to **completely float in a water depth of 0.95 m**. Smaller vehicles like the Toyota Yaris with weight of about 1.0 tonne are far more vulnerable due to their lower kerb weight. The **Toyota Yaris** tested in this investigation **completely floated in water 0.6 m deep**.

Results from this investigation have demonstrated that moving flood waters have significant momentum and can impart large hydrodynamic forces to vehicles exposed to the flow. This is not a surprising outcome. To provide some context, each **one (1) metre cube of water** (1 m by 1 m by 1 m box) of water **weighs one (1) tonne**. If a small car like a Toyota Yaris, which is

4.3 m long, is exposed to floodwaters **0.4 m deep** travelling at **1 m/s (3.6 km/h)**, which is less than walking pace, then the car is being impacted by one tonne of water every second. So the **force of the water** impacting the vehicle, even at walking pace, **is similar to being in a collision with another small car** every second. If the water is moving at walking pace of **2m/s (7.2 km/h)** the **force of the water** is similar to a **collision with a 4WD every second**.

In fast moving flows, which can be upwards of three (3) to four (4) metres per second when flows pass over bridges and causeways, this means that the smallest vehicles (see Table 7-1) on Australian roads can become vulnerable when the flow is above the vehicle floor level in flood depths as shallow as 0.15 m (15 cm).

Many 4WD manufacturers highlight the ability of 4WD vehicles to operate in water. For example, the Ford Ranger is advertised as being able to negotiate water up to depths of 0.8 m (<http://www.motoring.com.au/new-ranger-in-deep-water-24397/> accessed 21 March 2017). The alarming aspect of this claim is that the testing conducted for this investigation showed that in water 0.8m deep, a 4WD vehicle would become unstable and vulnerable to being washed off a bridge or causeway in flow travelling **at about walking pace** (i.e. 2 m/s or 7.2 km/h).

Since the force of flowing water is proportional to the velocity squared (see equation 3), small increases in flow speed result in significant increases in the force the flow can impart. Observations of flood flows in the field note that they rarely pass over a roadway steadily. Rather, observations of real floods show that flows can change rapidly increasing and decreasing in both depth and speed in a 'surging' or random 'pulsing' manner. In an operational context, these often rapidly changing flow conditions make it very difficult to determine whether a floodplain crossing is safe or not.

For flow depths that impact the body of the vehicle, there is no simple, safe guidance for vehicle stability. Flows impacting the vehicle body may be safe for low depths and low velocities, but it is highly variable from vehicle to vehicle, and as noted above, judgement of flow velocity (and often depth) is difficult in real world situations.

In a flood emergency, the best advice remains to simply avoid driving in floodwaters.

7.4.2 Comparison with existing flood hazard curves

The testing conducted for this investigation provides the opportunity to review the flood hazard curves for vehicles derived for floodplain planning and emergency management, such as the hazard curves published in ARR P10 (Shand et al., 2011) and AEMI Handbook 7 (2014). These hazard curves provide a means for floodplain and emergency managers to classify flood behaviour, as described by measured or predicted flood depths and flood flow velocities, with a 'danger' rating. The hazard rating for vehicles has been in the past, been quantified by the best estimate of flow conditions that would cause a vehicle to become unstable in floodwaters and wash away downstream. An example of a set of hazard curves from AEMI Handbook 7 (2014) is provided in this report as Figure 2-1.

Consideration of the prototype instability force testing and model scale hydrodynamic testing in combination enables flow instability threshold conditions for vehicles to be developed and compared to existing flood hazard curves. This assessment requires estimation of suitable values for coefficients in the governing equations described in Section 4.2. In particular, the analysis

requires the adoption of values for the coefficient of drag (C_D) for the partially submerged vehicle and the coefficient of friction (μ) for the vehicles tyres.

A conservative effective coefficient of friction of 0.3 was adopted on the basis of the discussion in Section 4.2.1 and the ratios summarised in Table 5-2. This value was adopted using similar reasoning to the findings of Bonham and Hattersly (1967) who considered a braking force coefficient of 0.5 on a worst case scenario of "a smooth causeway surface on a wet country road" with adjustments made for a reduced sideways force compared with breaking force (10%), the reduced slipping force compared with peak breaking force (20%), and a further reduction due to debris that may become caught under the wheels (20%). This results in an adopted coefficient of friction of 0.3.

An adopted coefficient of drag of 2.0 provides a conservative value based on the range of measured values provided in Section 6 as summarised in Table 6-1. Uplift is assumed to be zero, but can be considered to be accounted for in the conservative value of coefficient of drag.

A comparison of data derived from the testing on the basis of these adopted coefficients with the currently adopted curves from ARR P10 is provided in Figure 7-3 for the Toyota Yaris (representative of small cars) and in Figure 7-4 for the Nissan Patrol (representative of large 4WD vehicles).

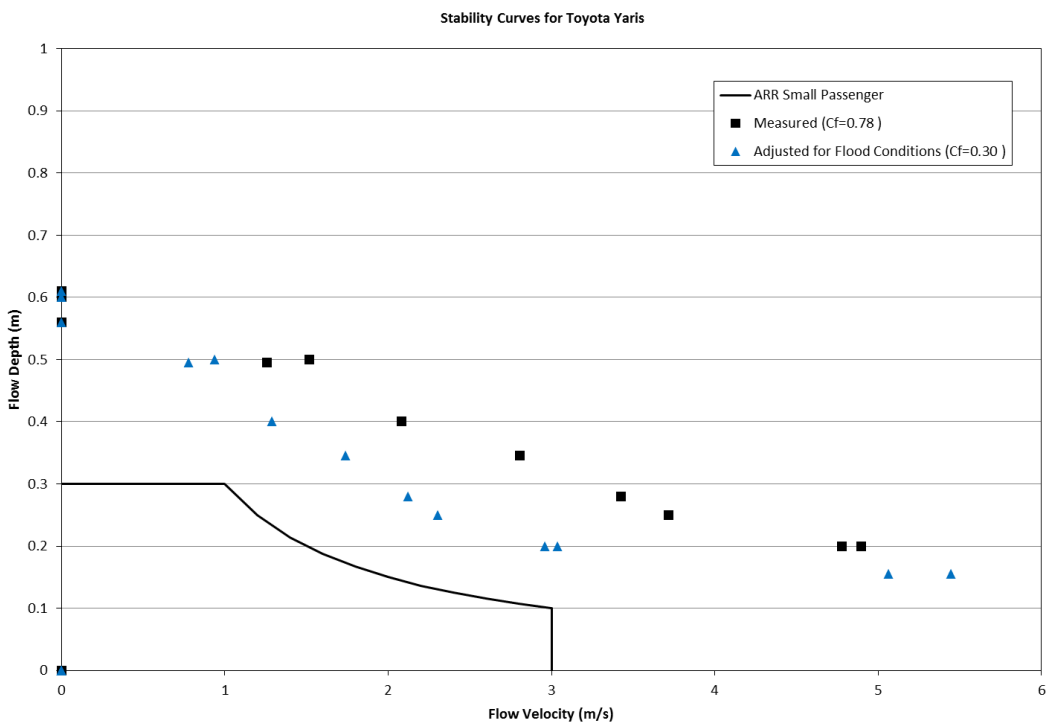


Figure 7-3: Stability Curve for a Toyota Yaris based on full scale traction tests, upper limits for the Coefficient of Drag $C_D = 2.0$ based on scale testing, and points scaled to a flood condition Coefficient of Friction of 0.3

At face value, the test results presented in Figure 7-3 indicate that the Toyota Yaris is more stable than the interim vulnerability threshold condition for a 'small passenger vehicle' from ARR P10 expressed in terms of a flow velocity times depth product ($v.D$). The interim adopted

hazard threshold for a small passenger vehicle from ARR p10 is $v.D = 0.3$ whereas the data from the testing of the Toyota Yaris results in a $v.D$ threshold of approximately 0.5.

Similarly, the test results presented in Figure 7-4 indicate that the Nissan Patrol 4WD is significantly more stable than the interim vulnerability threshold for a 'large 4WD vehicle' from ARR P10 of 0.5. The hazard threshold estimated from the test results for the Nissan Patrol has a factor of safety of more than two (2) times the ARR P10 interim hazard guidelines.

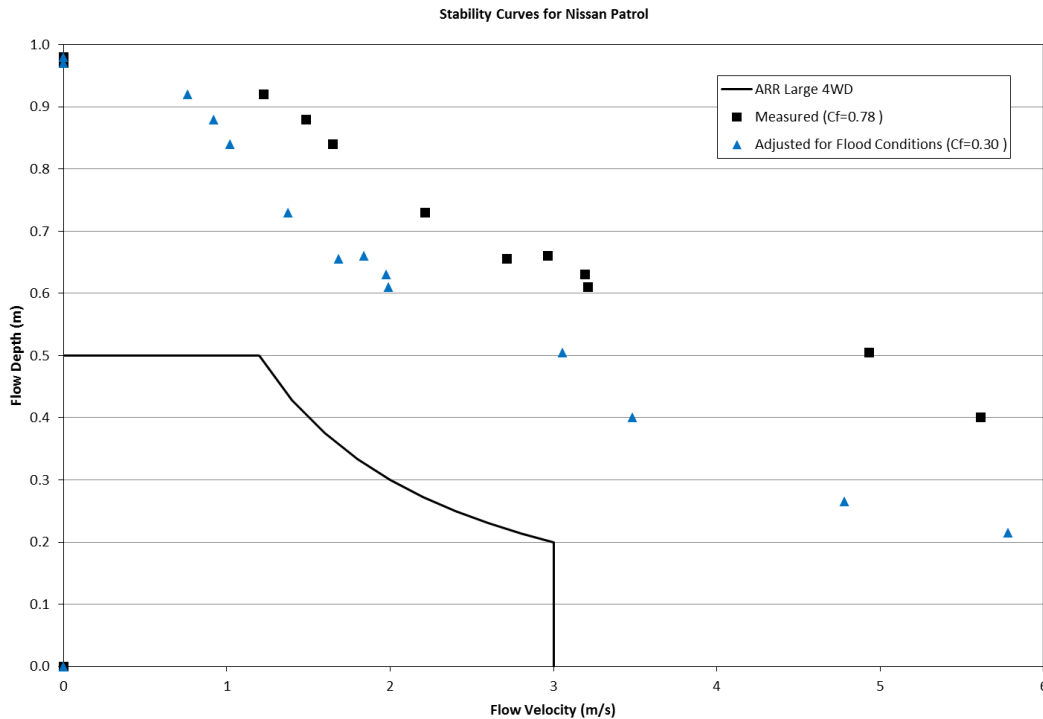


Figure 7-4: Stability Curve for a Nissan Patrol based on full scale traction tests, upper limits for the Coefficient of Drag $C_D = 2.0$ based on scale testing, and points scaled to a flood condition Coefficient of Friction of 0.3

There are, however, a range of limitations and in the testing regime which need to be carefully considered when interpreting the test results from this investigation into a form suitable for classifying flood hazard behaviour for floodplain planning or emergency planning and operations.

Firstly, when considering the vulnerability classification for small passenger vehicles, the Toyota Yaris, while small, is far from the smallest, most vulnerable vehicle on Australian roads. Table 7-1 lists a number of vehicles that have lower road clearance and lighter kerb weight than the Toyota Yaris.

Similarly, while the Nissan Patrol might be considered representative of 'large 4WD vehicles' there are numerous smaller 4WD vehicles that are lighter and have less ground clearance in this class of vehicles. 4WD vehicles are also more likely to have larger tyres for off-road driving that provided added buoyancy to the vehicles.

Secondly, there are a number of mitigating factors within the testing program that make it sensible to apply a conservative interpretation of the results for a real-world application. These

relate predominantly to the interpretation of the hydrodynamic flow conditions from the 1:18 scale modelling to real world conditions and include:

- The laboratory testing was conducted in ideal conditions, with regular channel dimensions and steady flow. These conditions would rarely be encountered in real world conditions. In the real world, flows are often sediment laden and sometimes contain large debris both of which would increase the flow force on an exposed vehicle. Road surfaces in flood affected areas are also often uneven with potholes and loose gravel making full contact of all wheels on the submerged road surface problematic;
- Laboratory testing was completed with stationary vehicles. In real flood conditions, most cars will be driven into floodwaters and the act of rolling into the floodwaters may contribute additional uplift forces and an associated reduction in friction not accounted for in the testing;
- The impact of turbulent, pulsating or varying flows has not been considered in the testing but might often be prevalent in real world conditions, especially in flash flood conditions, and is likely important in initially destabilising a vehicle;
- The present test considered a simplified area for the drag force calculations. While the flow would increase in the close proximity of the vehicle, in the present test the cross-sectional area of the vehicle impacted by drag force was calculated based upon the flow depth measured upstream of the vehicle. This would have resulted in a proportionally larger flow velocity in the model and a reduced flow depth close to the vehicle;
- The changes to vehicle height and roll angle (loading and/or unloading of the suspension) due to buoyancy and side impact forces were not considered in the scale hydrodynamic tests;
- Uplift forces on the model scale stationary vehicle were not well represented in the testing, largely due to the magnitude of surface tension forces compared to the weight of the vehicle. In other words, when considering the vertical forces, the weight of the water raised by surface tension was significant compared with the uplift forces in the model.

In due consideration of these aspects of the testing program i.e. i) that the test vehicles are not representative of the most vulnerable vehicles in their class on Australian roads; and ii) that there are limitations with the absolute accuracy of the results in the testing program, it is appropriate that flood hazard thresholds for planning purposes remain conservative compared to the test data presented here.

On this basis, the authors recommend that the interim flood hazard threshold curves from ARR P10 summarised here as Table 7-2 for the two vehicle classes tested in this investigation be adopted for use in future floodplain management and emergency management.

Table 7-2: Proposed flood hazard thresholds for vehicle stability

Class of Vehicle	Length (m)	Kerb Weight (kg)	Ground Clearance (m)	Limiting Still Water Depth¹	Limiting High Velocity Flow Depth²	Limiting Velocity³	Equation of Stability
Small passenger	< 4.3	< 1250	< 0.12	0.3	0.15	3.0	$D.V \leq 0.3$
Large 4WD	> 4.5	> 2000	> 0.22	0.5	0.3	3.0	$D.V \leq 0.6$

¹ At velocity = 0 m/s; ² At velocity = 3 m/s; ³ At low depth

8. Conclusions

A study of vehicle stability in floodwater flows was conducted at UNSW Sydney WRL's laboratory's facilities incorporating full prototype scale testing of traction and buoyancy forces on a vehicle in static water, and hydrodynamic force measurement on 1:18 scale model vehicles.

The traction force tests conducted are novel in research on stability of vehicles, and show that traction decreases rapidly with depths above the vehicle's floor pan level. The testing confirmed that the rear wheels (wheels not weighted by the engine) lose traction far earlier than the front wheels.

Hydrodynamic testing showed that coefficients of drag for the vehicle in free surface water flows, perpendicular to the vehicle, are far higher than typical wind tunnel based aerodynamic drag coefficients. These are consistent with drag coefficients predicted by Hoerner (1965) for water surface piercing drag and complicated by the vehicle geometry and low depth to vehicle length ratios. The coefficient of drag varies non-linearly with the flow condition, but is generally within the range 1.2 and 2.0 for typical, dangerous conditions.

The test program and analysis presents a novel approach to the derivation of stability curves for vehicles in flood flows, by dissecting the forces that impact the vehicle, applying appropriate factors of safety, and evaluating vehicle stability directly from the stability balance equation.

Observations from the testing indicate that where floodwaters impact the body of the vehicle, the vehicle is at serious risk of losing traction and being washed downstream. Flows that do not impact the body of the vehicle (hitting the wheels only) are generally safe for that vehicle.

Analysis of results from this investigation showed that the subject test vehicles were more stable in flood flows than the flood hazard vulnerability thresholds typically applied for floodplain management and emergency management as documented by guidelines such as Australian Rainfall and Runoff Review Project 10 (ARR P10) (Shand et al., 2011) and AEMI Handbook 7 (2014).

However, mitigating factors described in this report, notably i) that the tested vehicles, while representative, were not the smallest in their vehicle class and ii) that controlled laboratory conditions need to be interpreted to uncontrolled real life flood conditions means that application of a level of conservatism on this study's results is warranted.

8.1 Recommendations

In the course of this investigation, numerous issues were encountered, which with the fullness of time and available funding, warrant further analysis.

These issues include:

1. Vehicles should primarily be tested with the vehicle oriented at or near perpendicular to the flow. Consideration for vehicles at other angles may be beneficial, but it is expected that the limiting case for vehicle vulnerability in floods is perpendicular to the flow;
2. Further research is required on the range of coefficients of drag for a range of vehicles in free surface water flow, preferably at prototype scale;

3. Effect of pulsating or turbulent flows. Eddies, turbulence and other variations in flow are likely to rock the vehicle from side to side on its suspension in floods, affecting the hydrodynamic drag and uplift, and traction forces. Further study on this effect is warranted.
4. One of the significant unknowns in vehicle stability is the coefficient of friction between tyres and the submerged road in flood conditions. While the coefficient of friction adopted in this study and others ($\mu = 0.3$) is conservative, a better understanding of the effect of various surface types and the effect of debris on the road on tyre friction would improve the accuracy of this study's outcomes.
5. Lifting of the vehicle (unloading the suspension) due to buoyancy was not considered in the scaled hydrodynamic tests. Similarly, the rolling of the vehicle on the suspension due to the side impact of the water was not considered in the scaled hydrodynamic tests. Both of these would have further impacts on both horizontal and vertical hydrodynamic forces on the vehicle. It is expected that a significantly larger scale would be required to correctly model these forces.
6. Testing of the model vehicle was conducted on a broad crested weir, resembling a typical road embankment, but only in a single location. It is recommended that testing be conducted across a range of distances downstream of the weirs upstream edge.

9. Acknowledgements

The authors of this report acknowledge the contribution of the NSW State Emergency Service and NSW Office of Environment and Heritage for their substantial funding of this investigation.

This research could not have progressed without the generosity of NRMA Insurance who provided the test vehicles at no cost to the investigation.

10. References

- AEMI. (2014) Australian Emergency Management Handbook: Managing the floodplain: best practice in flood risk management in Australia, (AEMI Handbook 7, 2014)
- Bird, G. and Scott W.J.O. (1936) *Studies in Road Friction, I. Road Surface Resistance to Skidding* D.S.I.R., Road Research Tech. Pap. No.1 H.M.S.O., 1936
- Bird, G. and Scott W.J.O. (1936) *Studies in Road Friction, II. An Analysis of the Factors Affecting Measurement* D.S.I.R., Road Research Tech. Pap. No.2 H.M.S.O., 1936
- Bonham, A.J. and Hattersley, R.T. (1967) *Low Level Causeways*, University of New South Wales, Water Research Laboratory, Technical Report No. 100, August 1967
- Bowen, W and Alexander, K. (2011) *Surface Piercing Drag in CFD*. In: *Proceedings of the ASME 30th International Conference on Ocean, Offshore and Arctic Engineering*. OMAE2011-49651
- Cox, R.J., Shand, T.D. and Blacka, M.J. (2010) Appropriate Safety Criteria for People in Floods. WRL Research Report 240. ARR Project No. 10, prepared for Institution of Engineers Australia. 22p
- DIPNR (New South Wales Government Department of Infrastructure, Planning and Natural Resources) 2005, Floodplain development manual: the management of flood liable land, Department of Infrastructure, Planning and Natural Resources, Sydney
- Gallaway, B M, Ivey, D L, Hayes, G, Ledbetter, W B, Olson, R M, Woods, D L and Schiller, R F Jr. (1979) *Pavement and Geometric Design Criteria for Minimising Hydroplaning*. Federal Highway Administration Report RHWA-RD-79-31. 296 p
- Gerard, M. (2006). *Tyre-road friction estimation using slip-based observers*. Master's thesis. Dept. Automatic Control, Lund University, Lund Sweden
- Gordon, A.D. and Stone, P.B. (1973) *Car Stability on Road Causeways*. WRL Technical Report No. 73/12. 5p + Appendices
- Haynes, K., Coates, L., Dimer de Oliveira, F., Gissing, A., Bird, D., van den Honert, R., Radford, D., D'Arcy, R, Smith, C. (2016) *An analysis of human fatalities from floods in Australia 1900-2015*. Report for the Bushfire and Natural Hazards CRC
- Haynes, K. and Gissing, A. (2016) *Flood deaths are avoidable: don't go in the water*. Macquarie University. <https://theconversation.com/flood-deaths-are-avoidable-dont-go-in-the-water-60615> published June 7, 2016 accessed 27 September 2016
- Hoerner, S.F., (1965) *Fluid-dynamic drag: practical information on aerodynamic drag and hydrodynamic resistance*. Midland Park, N.J.: Dr.-Ing. S.F. Hoerner
- International Federation of Red Cross and Red Crescent Societies (2015) *World disasters report*. Geneva, Switzerland
- Jonkman, S.N. (2005) *Global perspectives on loss of human life caused by floods*. *Natural Hazards*, 34 (2), pp.151-175

Kramer M., Terheiden K., and Wieprecht S. (2016) *Safety criteria for the trafficability of inundated roads in urban floodings*. In: *International Journal of Disaster Risk Reduction*, 17 pp. 77–84 <http://dx.doi.org/10.1016/j.ijdrr.2016.04.003>

Keller, R.J., and Mitsch, B. F., (1992) *Stability of Cars and Children in Flooded Streets In: International Symposium on Urban Stormwater Management (1992 : Sydney, N.S.W.)*. International Symposium on Urban Stormwater Management: Preprints of Papers. Barton, ACT: Institution of Engineers, Australia, 1992: 264-268. National conference publication (Institution of Engineers, Australia) ; no. 92/1. ISBN: 0858255472

Martínez-Gomariz, E., Gómez, M., Russo, B. and Djordjević, S. (2016) Stability criteria for flooded vehicles: a state-of-the-art review. *J Flood Risk Management*. doi:10.1111/jfr3.12262
Munson, B. R., Okiishi, T. H., Huebsch W. W. and Rothmayer A. P. (2013) *Fundamentals of Fluid Mechanics*. 7th edition

NSW SES (2016) *Flood safety warning following 300 flood rescues*. Web article: <http://www.ses.nsw.gov.au/news/76365/77179> accessed 27 September 2016

Oshikawa H., Oshima T. and Komatsu T. "Study on the Risk for Vehicular Traffic in a Flood Situation" (in Japanese). *Adv River Eng* 2011, 17, 461–466

Roads and Maritime Services (2012) *Vehicle Standards Information No. 5 Rev6 VSI No.5*

Shand, T.D., Cox, R.J., Blacka, M.J. and Smith, G.P. (2011) *Australian Rainfall and Runoff Revision Project 10: Appropriate Safety Criteria for Vehicles - Literature Review*. Australian Rainfall and Runoff Revision Project 10. Stage 2 Report. Prepared by the Water Research Laboratory. P10/S2/020. February 2011

Smith, G.P., Davey, E.K., and Cox, R.J. (2014) *Flood Hazard*. UNSW Australia Water Research Laboratory Technical Report 2014/07

Shu, C., Xia, J., Falconer, R.A. and Lin, B. (2011) "Incipient Velocity for Partially Submerged Vehicles in Floodwaters". *Journal of Hydraulic Research*, 49 (6), pp.709-717

Taborek, J.J. (1957) "Mechanics of Vehicles," *Machine Design*, May 30-Dec. 26

Toda K., Ishigaki T. and Ozaki T. (2012) "Experiment study on floating car in flooding." International Conference on Flood Resilience: Experiences in Asia and Europe, Exeter, UK, 2013, 6.

Xia, J., Teo, F.Y., Lin, B. and Falconer, R.A. (2011) "Formula of Incipient Velocity for Flooded Vehicles". *Natural Hazards*, 58 (1), pp.1-14

Xia J., Falconer R.A., Wang Y. and Xiao X. (2011) "New criterion for the stability of a human body in floodwaters." *J Hydraul Res* 2014, 52, 93–104. doi: 10.1080/00221686.2013.875073

Xia J., Falconer R.A., Xiao X. and Wang Y. (2013) "Criterion of vehicle stability in floodwaters based on theoretical and experimental studies." *Nat Hazards* 2013, 70, 1619–1630. doi: 10.1007/s11069-013-0889-2.

Wong J.Y, (1993) *Theory of ground vehicles*, 2nd ed.